bioRxiv preprint doi: https://doi.org/10.1101/2020.07.15.204859; this version posted May 20, 2021. The copyright holder for this preprint (which was not certified by peer review) is the author/funder, who has granted bioRxiv a license to display the preprint in perpetuity. It is made available under aCC-BY-NC-ND 4.0 International license.

Global transcriptional regulation by cell-free supernatant of *Salmonella* Typhimurium peptide transporter mutant leads to inhibition of intra-species biofilm initiation

Kasturi Chandra[1], Prerana Muralidhara[2,‡], Sathisha Kamanna[3], Utpal S. Tatu[3], Dipshikha Chakravortty[1,4,#]

[1]Department of Microbiology and Cell Biology, Indian Institute of Science, Bangalore, India.

[2]Department of Molecular Biology, Yuvaraja's College, Mysore, Karnataka, India.

[3]Department of Biochemistry, Indian Institute of Science, Bangalore, India.

[4]Centre for BioSystems Science and Engineering, Indian Institute of Science, Bangalore, India.

[‡]Present address: Molecular Biology and Genetic Unit, Jawaharlal Nehru Centre for Advanced Scientific Research, Bangalore, India

 # Corresponding author

Dipshikha Chakravortty

Email: dipa@iisc.ac.in

Telephone: +91 80 22932842

Keywords: *Salmonella* Typhimurium, Biofilm, flagella, H-NS, EPS, yjiY, oxidative stress

bioRxiv preprint doi: https://doi.org/10.1101/2020.07.15.204859; this version posted May 20, 2021. The copyright holder for this preprint (which was not certified by peer review) is the author/funder, who has granted bioRxiv a license to display the preprint in perpetuity. It is made available under aCC-BY-NC-ND 4.0 International license.

Abstract

Salmonella is a genus of widely spread Gram negative, facultative anaerobic bacteria, which is known to cause ¼th of diarrheal morbidity and mortality globally. It causes typhoid fever and gastroenteritis by gaining access to the host gut through contaminated food and water. *Salmonella* utilizes its biofilm lifestyle to strongly resist antibiotics and persist in the host. Although biofilm removal or dispersal has been studied widely, the inhibition of the initiation of *Salmonella* biofilm remains elusive. This study was conducted to determine the anti-biofilm property of the cell-free supernatant obtained from a carbon-starvation inducible proline peptide transporter mutant (Δ*yjiY)* strain. Our study shows that *Salmonella* Δ*yjiY* culture supernatant primarily inhibits biofilm initiation by regulating biofilm-associated transcriptional network. This work demonstrates that highly abundant proteases such as HslV and GrpE cleave the protein aggregates, whereas global transcription regulators H-NS, FlgM regulate expression of SPIs and flagellar genes. Relatively low abundances of flavoredoxin, glutaredoxin, thiol peroxidase etc. leads to accumulation of ROS within the biofilm, and subsequent toxicity. This work further suggests that targeting these oxidative stress relieving proteins might be a good druggable choice to reduce *Salmonella* biofilm.

Importance

The enteric pathogen *Salmonella* forms biofilm in the internal organs of asymptomatic carriers, and on abiotic surfaces that leads to contamination of food and water. Biofilms are highly drug-resistant life forms that also helps in host immune evasion. Therefore, recent insurgence of drug tolerant strains necessitates development of biofilm inhibitory strategies, and finding novel

bioRxiv preprint doi: https://doi.org/10.1101/2020.07.15.204859; this version posted May 20, 2021. The copyright holder for this preprint (which was not certified by peer review) is the author/funder, who has granted bioRxiv a license to display the preprint in perpetuity. It is made available under aCC-BY-NC-ND 4.0 International license.

42 druggable targets. In this study we investigated the bioactive molecules present in the cell-free
43 supernatant of a biofilm deficient strain of *Salmonella* Typhimurium that inhibit biofilm
44 initiation by the wildtype strain. Further we showed that the supernatant treatment leads to
45 virulence defect *in vivo*. Collectively, our results suggest a comprehensive view of virulence
46 regulation in *Salmonella* by the cell-free supernatant of the biofilm deficient strain.

47

48 **Introduction**

49 *Salmonella* is one of the most common foodborne pathogens that causes one of the 4 major
50 diarrheal diseases, salmonellosis (1, 2). The biofilm life form of this bacteria makes it a hardy
51 human pathogen that can survive several weeks in a dry environment and many months in water
52 (3). A biofilm refers to a community of bacteria adherent to a biotic/abiotic substratum, held
53 together by its secreted extracellular polymeric substances. Biofilms are highly resistant to
54 antibiotics, disinfectants etc. and biofilms on medical devices, catheters, implants are a major
55 cause of hospital acquired infections (4, 5). Recent reports suggest that *Salmonella* can form
56 biofilm on the gall bladder, leading to chronic infection (6, 7). The major constituents of
57 *Salmonella* biofilm are curli, cellulose and BapA. Curli facilitates intercellular and cell to surface
58 interactions, cellulose enables long range contact and provides characteristic stickiness to the
59 biofilm and BapA strengthens curli interactions and stabilizes the biofilm (8). A major cue for
60 biofilm formation is nutritional stress. Previously we found that the deletion of carbon starvation
61 inducible gene, *yjiY*, leads to deficiency in biofilm formation (9). Antibiotic stress, DNA
62 damage, cold stress, acid stress etc. can also regulate the transcription of *yjiY* gene (10-12). In *S.*
63 Typhimurium, YjiY is known to regulate virulence by affecting flagellar class III genes, and the
64 deletion of *yjiY* leads to reduced colonization in mice (9, 13), and upregulation of the virulence

bioRxiv preprint doi: https://doi.org/10.1101/2020.07.15.204859; this version posted May 20, 2021. The copyright holder for this preprint (which was not certified by peer review) is the author/funder, who has granted bioRxiv a license to display the preprint in perpetuity. It is made available under aCC-BY-NC-ND 4.0 International license.

65 factor *mgtC*, leading to biofilm deficiency (14). This could indicate the possible role of YjiY in
66 survival and defense against host induced stress in bacteria.

67 Recent studies corroborate that various culture supernatants of commensal bacteria can inhibit
68 colonization and biofilm formation by their pathogenic counterparts. This inhibitory activity of
69 culture supernatants can be seen across Gram positive, and Gram negative bacteria as well as
70 across kingdoms. Iwase *et al.* showed that *Staphylococcus epidermidis* Esp inhibits biofilm
71 formation and nasal colonization by pathogenic *Staphylococcus aureus* (15). In another study,
72 probiotic *Escherichia coli* Nissle (EcN) inhibited biofilm formation in pathogenic EHEC, by a
73 secreted bifunctional (protease and chaperone) protein DegP (16). There are various other modes
74 of interspecies biofilm regulation such as biofilm dispersal proteins (17), indole-mediated
75 biofilm regulation (18), quorum sensing molecules, and antimicrobial peptides (19). The
76 inhibition can also be interkingdom, such as *Aspergillus* biofilm inhibition by *Pseudomonas*
77 culture supernatants (20). While there are a few strategies to deal with preformed biofilms (21,
78 22), the inhibition of biofilm initiation is comparatively less explored in human pathogens. In our
79 lab we found that *Salmonella* WT could not form biofilm when cocultured with Δ*yjiY* strain. This
80 study was designed to investigate the novel biofilm inhibitory activity of biofilm deficient strain
81 *Salmonella* Typhimurium Δ*yjiY*.

82 In this study, we are reporting a novel mechanism of biofilm initiation inhibition by a complex
83 transcriptional regulatory network. This complex network causes adhesion impairment, flagellar
84 motility inhibition, cleavage of protein aggregates and quorum sensing inhibition. Furthermore,
85 we have shown that STM Δ*yjiY* supernatant can also inhibit biofilm formation by *E. coli*. We
86 have also shown that the supernatant treatment can impair the invasion of the pathogen in the *C.*
87 *elegans* gut, thus reducing its virulence.

bioRxiv preprint doi: https://doi.org/10.1101/2020.07.15.204859; this version posted May 20, 2021. The copyright holder for this preprint (which was not certified by peer review) is the author/funder, who has granted bioRxiv a license to display the preprint in perpetuity. It is made available under aCC-BY-NC-ND 4.0 International license.

Results

Salmonella ΔyjiY culture supernatant inhibits WT biofilm formation

To understand the biofilm inhibitory property of STM Δ*yjiY* culture supernatant, we inoculated WT bacteria in biofilm inducing low salinity media with or without the culture supernatant of different strains. The Δ*yjiY* bacterial culture supernatant exhibited the biofilm inhibitory property (**Fig. 1A**), which was absent in the supernatant of the strain where *yjiY* was trans-complemented in a plasmid (STM Δ*yjiY*:pQE60-*yjiY*). Previous study showed that Δ*yjiY* is a biofilm deficient strain (14). To check whether the biofilm inhibitory property is specific to Δ*yjiY* supernatant, we inoculated WT strain with biofilm deficient strain Δ*csgD* (**Fig. S1A**). We observed inhibition only in the case of Δ*yjiY* supernatant indicating that the inhibitory molecules are unique to the Δ*yjiY* secretome, and are independent of the activity of CsgD. To further validate that the inhibition is a cell-free phenomenon, we inoculated WT bacteria along with either live cells of other strains along with spent culture media (coculture), supernatant-free cell pellets, cell free supernatant, or whole cell lysate, and quantified the biofilm on solid-liquid-air interface. Although Δ*yjiY* showed significant inhibition of biofilm formation in all the setups, the maximum inhibition was observed with Δ*yjiY* culture supernatant (**Fig. 1B**). The supernatants were concentrated using an Amicon ultra filter device and total protein was quantified. We found that minimum biofilm inhibitory concentration (**MBIC**; minimum concentration of total protein required to inhibit biofilm formation by WT strain) falls between 15-20 ng protein/ml (**Fig. 1C**), therefore we used supernatant containing 20 ng protein/ml of supernatant for further experiments. We did not find any difference in the growth (**Fig. S1B**), suggesting that the supernatant lacks any bactericidal or bacteriostatic properties. Interestingly, we observed slower, yet longer exponential growth after supernatant treatment (**Fig. S1C**). To determine whether the

bioRxiv preprint doi: https://doi.org/10.1101/2020.07.15.204859; this version posted May 20, 2021. The copyright holder for this preprint (which was not certified by peer review) is the author/funder, who has granted bioRxiv a license to display the preprint in perpetuity. It is made available under aCC-BY-NC-ND 4.0 International license.

secretion of the inhibitory component(s), is dependent on the culture media, we grew the bacteria in minimal media (M9 media supplemented with 0.5% glucose) that exerts nutrition stress and used the supernatant to treat WT bacteria. We observed that the biofilm inhibitory molecule(s) were active even in minimal media (**Fig. 1D**), suggesting that the production of the inhibitory molecule(s) is not dependent on the nutritional condition and is an intrinsic property of the Δ*yjiY* strain. Additionally we checked the temporal expression or accumulation of the inhibitory component(s) by inoculating the WT strain with culture supernatant harvested from 2, 3, 4 and 5 day old Δ*yjiY* cultures. Our results suggest that the optimum concentration of the inhibitory component(s) is/are reached after 3 days of growth (**Fig. S1D**), which remains unchanged on the 4^{th}-5^{th} days of growth. Therefore, we used filtered culture supernatant from 3 day old Δ*yjiY* culture for further experiments.

Δ*yjiY* culture supernatant weakens the WT biofilm and interferes with cell structure

The characteristic EPS components are cellulose (produced by *bcsA* encoded cellulose synthase), curli fimbriae (encoded by *csgAB*), BapA and LPS (23). We observed a significant reduction of the EPS bound Congo red fluorescence intensity (**Fig. 2A, S2A**) and biofilm thickness (**Fig. S2B, S2C**) upon Δ*yjiY* supernatant treatment. We also found that Δ*yjiY* supernatant treatment significantly reduced the strength of the biofilm pellicle (**Fig. S2D, S2E, 2B**) than that of untreated or WT supernatant treated samples. SEM and AFM analysis of the biofilm surface showed that the Δ*yjiY* supernatant treated biofilms lack the characteristic dome shape of a proper biofilm (**Fig. 2C, S2F**). We also noticed that the median cell length increased upon Δ*yjiY* supernatant treatment (1.58$\pm$0.30 µm) as compared to the untreated WT cells (1.38$\pm$0.34 µm) (**Fig. 2D, 2E, S2G**), hinting towards the presence of multiple regulatory components in the Δ*yjiY* supernatant that can modulate multiple phenotypic effects.

bioRxiv preprint doi: https://doi.org/10.1101/2020.07.15.204859; this version posted May 20, 2021. The copyright holder for this preprint (which was not certified by peer review) is the author/funder, who has granted bioRxiv a license to display the preprint in perpetuity. It is made available under aCC-BY-NC-ND 4.0 International license.

The active molecule(s) is/are protein(s)

Previous studies have shown that secreted components from some bacteria can inhibit biofilm formation by the wild type strain or closely related species (15, 16, 20). To delineate the chemical nature of the inhibitory molecule(s) present in Δ*yjiY* supernatant, we treated the supernatant with chemical agents, such as a divalent cation chelator (EDTA), protease (Proteinase K), protease inhibitor (PMSF), RNase and DNase and quantified the biofilm inhibition. We found that upon pre-treatment with different concentrations of EDTA, the inhibitory property remained intact. Interestingly, 10 mM EDTA enhanced biofilm formation with both treated and untreated WT strain (**Fig. 3A**). Since EDTA is known to chelate divalent cations and inhibit a few proteases at higher concentrations (24-27), our data signify the requirement of divalent cations and/or active proteases for biofilm inhibition. Upon treating the supernatants with 20 mg/ml Proteinase K, the ability of Δ*yjiY* supernatant to inhibit biofilm formation was significantly reduced, suggesting that the inhibitory molecule(s) are protein(s) (**Fig. 3B**). Since the activity of many proteins is sensitive to even small changes in pH and temperature, we checked the activity of Δ*yjiY* supernatant at different pH and temperatures. Surprisingly, we found that the active component(s) is/are heat stable at 65 ^{o}C and 95 ^{o}C temperatures (**Fig. 3C**) and stable over a wide range of acidic and alkaline pH (**Fig. 3D**), although there was a small reduction in biofilm inhibition at pH 9.0. As recent studies show that several small noncoding RNAs regulate biofilm formation and other virulence traits in *Vibrio cholerae* and *Pseudomonas aeruginosa* (28, 29), we tested the stability of the component(s) after treating the supernatant with RNase. Although the inhibition was lost upon RNase treatment and incubation at 37^{o}C, we found a similar loss of inhibition with only heating the supernatant at 37^{o}C (**Fig. S3A**), suggestive of the heat, rather RNase treatment, to be the reason for the loss of

bioRxiv preprint doi: https://doi.org/10.1101/2020.07.15.204859; this version posted May 20, 2021. The copyright holder for this preprint (which was not certified by peer review) is the author/funder, who has granted bioRxiv a license to display the preprint in perpetuity. It is made available under aCC-BY-NC-ND 4.0 International license.

inhibition. We also fractionated the supernatant using an Amicon 3k MWCO ultra filter device, and we found that the active component(s) of Δ*yjiY* supernatant is/are >3kDa molecular weight (**Fig. S3B**), quashing the role of small molecules and ions in biofilm inhibition by Δ*yjiY* supernatant. Since the inhibitory activity was abolished upon proteinase treatment, we attributed the inhibition to protein components and quantified the total protein for further experiments.

Active molecules inhibit biofilm only during the initial phases, and cannot disrupt mature biofilm

To determine the effect of the active molecule on mature biofilm, we treated mature biofilm pellicles with the supernatants and checked for dispersion. Our results showed that the Δ*yjiY* supernatant could not disrupt pre-formed biofilm, hinting towards the effect of the active molecule(s) on biofilm initiation (**Fig. 4A**). To determine whether the supernatant treated WT cells remained biofilm defective in the absence of the inhibitory molecules, the Δ*yjiY* supernatant treated WT cells were re-inoculated in biofilm medium without the supernatant, and monitored for pellicle formation. We observed that the inhibition was diminished in the absence of the supernatant (**Fig. 4B**), although the defect reappeared when these cells were re-treated with the inhibitory supernatant. Together our data suggest that supernatant mediated initial molecular reprogramming is required for biofilm inhibition, and that inhibitory molecules do not alter the inherent biofilm forming ability of the WT cells.

The inhibitory molecules impair flagella-mediated initial attachment to abiotic surfaces

Salmonella biofilm formation can be divided into 4 distinct steps, (i) initial attachment to the abiotic surface, (ii) secretion of adhesive components, (iii) maturation and (iv) dispersion of biofilm upon relief of the stress (30). Since biofilm initiation was inhibited and retained beyond

bioRxiv preprint doi: https://doi.org/10.1101/2020.07.15.204859; this version posted May 20, 2021. The copyright holder for this preprint (which was not certified by peer review) is the author/funder, who has granted bioRxiv a license to display the preprint in perpetuity. It is made available under aCC-BY-NC-ND 4.0 International license.

72 hours, we checked the expression of biofilm-associated genes (*csgD, bcsA, fliC*), SPI-1 effectors (*invF, sopD)* and virulence factors (*phoP, sodA, mgtC*) from untreated or treated WT cells, 72 hours post inoculation. We found that *csgD, bcsA, fliC* and *invF* expression was significantly downregulated in Δ*yjiY* supernatant treated WT cells (**Fig. 4C**). Since, flagella-mediated initial attachment initiates biofilm formation (31, 32), we investigated the effect of Δ*yjiY* supernatant on flagellar motility. We observed that Δ*yjiY* supernatant treatment significantly reduced both swimming and swarming motility (**Fig. 4D, 4E** and **S4A**), indicating a flagella-mediated motility defect. We further observed the downregulation of *fliC* occurs as early as 4-6 hours post inoculation with the Δ*yjiY* supernatant (**Fig. S4B**). Interestingly, we observed an increase in *fliC* expression at 12 hours post inoculation. We reasoned that adhesion deficiency arises from the sequential effect of the initial downregulation of *fliC,* followed by an increase in the planktonic population. SEM analysis showed that Δ*yjiY* supernatant treated bacteria had significantly fewer flagella (**Fig. 4F, S4C**). Altogether, these results indicate a defect in flagella-mediated initial attachment of the bacteria, sets the course for biofilm deficiency.

Δ*yjiY* supernatant reduces adhesion and virulence of *Salmonella* both *in vitro* and in *C. elegans* gut

Initial attachment of *Salmonella* on the host gut epithelial cells requires swimming through the mucus layer (33). SPI1 encoded Invs, Sops and Sips are important in initial invasion (34). Since Δ*yjiY* supernatant treatment downregulated *invF* and *sopD* expression, we checked the infectivity of the supernatant treated cells in mammalian intestinal epithelial cells, Int407. Invasion assay shows that Δ*yjiY* supernatant treated cells are defective in initial invasion, although these cells showed significantly higher intracellular proliferation than the untreated cells (**Fig. 5A** and **5B**), suggesting that the Δ*yjiY* supernatant only makes WT cells invasion defective by inhibiting

bioRxiv preprint doi: https://doi.org/10.1101/2020.07.15.204859; this version posted May 20, 2021. The copyright holder for this preprint (which was not certified by peer review) is the author/funder, who has granted bioRxiv a license to display the preprint in perpetuity. It is made available under aCC-BY-NC-ND 4.0 International license.

flagella-mediated adhesion. To check the infectivity of the Δ*yjiY* supernatant treated cells in a systemic condition, we fed young adult *C. elegans* N2 worms RFP-STM-WT bacteria and quantified gut colonization. The micrograph images and CFU analysis show that Δ*yjiY* supernatant treated RFP-STM-WT cells were able to colonize the gut lumen when fed continuously, but did not persist (**Fig. 5C, 5D, 5E**). Therefore, our data suggest that Δ*yjiY* supernatant treatment impairs *in vitro* invasion and *in vivo* colonization.

Inhibitory molecules impede biofilm formation in closely related species

We next checked the effectiveness of STM Δ*yjiY* supernatant on the biofilms of common human pathogens. We inoculated *E. coli* DH5α, *Pseudomonas aeruginosa* PA01, *Klebsiella pneumoniae, and Staphylococcus aureus* wild-type strains with STM WT supernatant, and STM Δ*yjiY* supernatant, and quantified the biofilm. We found that the STM Δ*yjiY* supernatant significantly inhibited only *E. coli* DH5α biofilm which is regulated by CsgD (**Fig. 5F**). Therefore, we concluded that the Δ*yjiY* supernatant can cross-react with closely related Enterobacteriaceae, *E. coli*, but is not effective against distant members such as *Klebsiella pneumoniae* or different family (*Pseudomonas aeruginosa*) or phylum (*Staphylococcus aureus*).

The active components are primarily global transcription factors that regulate multiple cellular processes

To further identify the biofilm inhibitory molecule(s), concentrated supernatants from WT and Δ*yjiY* cultures were resolved on 10% SDS-PAGE. After colloidal CBB staining, we clearly visualized 14 differential bands in Δ*yjiY* supernatant compared to WT supernatant (**Fig. 6A**). We next analyzed the secretome in LC Q-TOF MS/MS. Among the 244 proteins, 188 proteins were present in both supernatants at differential levels, while 38 and 58 proteins were enriched in the

bioRxiv preprint doi: https://doi.org/10.1101/2020.07.15.204859; this version posted May 20, 2021. The copyright holder for this preprint (which was not certified by peer review) is the author/funder, who has granted bioRxiv a license to display the preprint in perpetuity. It is made available under aCC-BY-NC-ND 4.0 International license.

WT supernatant and Δ*yjiY* supernatant, respectively (**Fig. 6B**). These proteins may have resulted from cell lysis during growth or they were secreted in the supernatant via an active secretion system. After careful data-mining, among the proteins found only in Δ*yjiY* supernatant (**Table S1**), probable transcriptional regulatory protein YebC, anti-sigma28 factor FlgM, a serine protease inhibitor ecotin and transcription termination/anti-termination protein NusG were selected for further analysis. Many transcriptional regulators (H-NS, Rnk, StpA), cold shock proteins (CspE, CspC), chaperones GrpE, ATP-dependent protease HslV, proteins related to oxidative stress and iron homeostasis (FldA, SodB, YdhD, Tph and Ftn, Bcp, Bfr, respectively) were differentially present in both supernatants (**Table S2**). Additionally, we treated STM WT cells with purified ecotin, HNS, and NusG (**Fig. S5**), to delineate the effect of each of these proteins. Interestingly, the fractions containing monomeric ecotin and NusG, as well as homodimeric HNS (**Fig. S6A, S6B**), showed biofilm inhibition similar to that of Δ*yjiY* supernatant, whereas the buffer (50mM Tris) treated WT cells did not have biofilm defect (**Fig. 6C**). Together, our data suggest that Δ*yjiY* supernatant perturbs various cellular processes leading to biofilm defect by complex transcriptional regulation (**Fig. 6D**).

Discussion

Salmonella forms biofilm to evade host defense, colonize in host, persist in asymptomatic host, and transmit to a new host (35). The transition from planktonic to biofilm mode depends upon various stress factors. The master regulator CsgD controls the production of EPS components such as cellulose, tafi (curli fimbriae) etc. by regulating AdrA. BapA is important both for biofilm production and attachment to intestinal epithelium (36). In this study we have shown how metabolic stress determines the fate of the infectious WT strain. From preliminary data, we found that coculture of STM WT and Δ*yjiY* led to biofilm defect in the WT strain. Although

bioRxiv preprint doi: https://doi.org/10.1101/2020.07.15.204859; this version posted May 20, 2021. The copyright holder for this preprint (which was not certified by peer review) is the author/funder, who has granted bioRxiv a license to display the preprint in perpetuity. It is made available under aCC-BY-NC-ND 4.0 International license.

various studies have shown that interspecies and intraspecies biofilm inhibitions exist in nature (15, 20, 37), in *Salmonella,* this phenotype is novel. Therefore, we carried out experiments to understand the underlying mechanism.

In this study, we found that biofilm inhibition was unique to Δ*yjiY* supernatant and the inhibition was reversed when WT cells were treated with culture supernatant from the complement strain (STM Δ*yjiY*:pQE60-*yjiY*). Although we observed that the Δ*yjiY* supernatant had only a biofilm inhibitory effect and lacked bactericidal properties (as observed from the growth analysis), STM WT cells showed delayed yet prolonged exponential growth upon supernatant treatment. Furthermore, the exopolysaccharide cellulose was sparse in the biofilm of Δ*yjiY* supernatant treated WT cells. Since only cellulose mutant *Salmonella* Typhimurium was proficient in adhering to tumour cells (38), our data imply the presence of multiple inhibitory factors involved in the inhibition by the supernatant. While incubation of Δ*yjiY* supernatant at 37˚C was found to reduce the inhibition, heating at 65˚C and 95˚C enhanced the inhibition, indicating that the inhibitory molecules might be heat-shock proteins or high temperature inducible stress proteins. Fascinatingly we observed that the effect of the inhibitory molecules is temporary, and they do not cause any genetic change to alter the inherent biofilm forming competency of the WT cells. Δ*yjiY* supernatant was also found to exert its anti-biofilm activity only when administered at the beginning of biofilm formation, suggesting a modification in the complex network through which biofilm develops. In the Δ*yjiY* supernatant treated WT cells, the expression of biofilm genes and virulence genes was reduced significantly. *sodA* downregulation suggests that these cells are prone to ROS assault. A previous study from our group showed that YjiY depletion upregulates *mgtC* leading to biofilm defect (14). Interestingly, we observed downregulation of *mgtC*, implying that biofilm inhibition by Δ*yjiY* supernatant and the inherent biofilm defect of

bioRxiv preprint doi: https://doi.org/10.1101/2020.07.15.204859; this version posted May 20, 2021. The copyright holder for this preprint (which was not certified by peer review) is the author/funder, who has granted bioRxiv a license to display the preprint in perpetuity. It is made available under aCC-BY-NC-ND 4.0 International license.

the Δ*yjiY* strain follow different mechanisms. The *ΔyjiY* supernatant treated WT cells showed significantly less invasion in Int407 cells. It was recently proposed that *Salmonella* persists in *C. elegans* gut by forming biofilm (39). Δ*yjiY* supernatant treated WT cells showed a concomitant reduction in colonization in the worm gut, suggesting an *in vivo* biofilm defect. We also observed the absence of flagella and other protein aggregates upon Δ*yjiY* supernatant treatment, leading to defects in cell aggregate formation and biofilm initiation. While there was a temporal increase in *fliC* in Δ*yjiY* supernatant treated WT cells, these cells exhibited defective motility after 72 hours of treatment, further validating the importance of flagella-mediated motility in the initial attachment of the bacteria to the substratum. Interestingly, we found that STM Δ*yjiY* supernatant effectively inhibited *E. coli* biofilm formation. Although *Salmonella* diverged from *E. coli* by acquiring virulence-associated genes, they share many evolutionarily conserved cellular pathways (40-42). Therefore this observation reiterates that the inhibitory effects are more profound among closely related species. In the proteomics analysis of the Δ*yjiY* supernatant, we specifically detected three potential inhibitory candidates: proteinase K sensitive ecotin (43), anti-sigma28 factor FlgM (a negative transcriptional regulator of class III flagellar genes (44, 45)) and YebC (negatively regulates quorum sensing in *Pseudomonas aeruginosa* PA01 (46)). The abundance of FlgM correlates with the absence of flagella in the Δ*yjiY* supernatant treated WT cells. NusG works synergistically with the global transcriptional regulator H-NS, which binds specifically to AT-rich SPIs in the *Salmonella* genome and represses those genes (47, 48). Interestingly, in *E. coli*, H-NS has been linked to the cell cycle, since the cells attempt to optimize spatial H-NS concentration by maintaining a constant ratio of H-NS to chromosomal DNA in the cell (49), which might explain the increase in cell length after Δ*yjiY* supernatant treatment. HslV, a heat-inducible ATP-dependent protease subunit of a proteasome-like degradation complex (50) and GrpE, which is involved in removal of protein aggregates leading

bioRxiv preprint doi: https://doi.org/10.1101/2020.07.15.204859; this version posted May 20, 2021. The copyright holder for this preprint (which was not certified by peer review) is the author/funder, who has granted bioRxiv a license to display the preprint in perpetuity. It is made available under aCC-BY-NC-ND 4.0 International license.

to unsuccessful biofilm formation (51) were found in higher abundance in Δ*yjiY* supernatant. Doyle *et al*.(52) showed that excess GrpE inhibits the interaction between DnaK and the regulatory protein, RepA. Since RepA helps maintain the plasmid copy number in *E. coli* (53), inactivation of RepA might explain cell elongation upon Δ*yjiY* supernatant treatment. While protein aggregation is necessary during initial attachment of the bacteria to an abiotic surface, upon maturation, proteolytic activity of several proteases helps in dispersal of biofilm (54). Presence of a protease inhibitor, such as ecotin, might hinder this process, leading to dysregulation of biofilm maturation and dispersion. Although several moonlighting functions have been demonstrated for mycobacterial superoxide dismutase and DnaK in modulating host response (55), any such activity for other hits remains elusive.

Oxidative stress proteins such as flavoredoxin, SodB, glutaredoxin, thiol peroxidase (Tph), and thioredoxin-dependent thiol peroxidase (Bcp) were less abundant in Δ*yjiY* supernatant, among which Tph and SodB help reduce oxidative stress in STEC biofilm (56). In *E. faecalis*, Tph is required for the *in vitro* oxidative stress response and survival inside murine macrophages (57). Iron availability has been shown to both positively and negatively regulate biofilm formation through complex network systems (58). Although high Fe can lead to ROS production, Kang and Kirienko suggested that iron uptake and homeostasis are essential for successful biofilm formation in *Pseudomonas aeruginosa* (59). The Fe-storage proteins bacterioferritin (Bfr) and ferritin A (Ftn), required to prevent ROS generation via the Fenton reaction and DNA damage, are functionally very large proteins with a core to accommodate 3000 Fe atoms. Fe-rich conditions induce *E. coli* FtnA and Bfr due to loss of repression by small RNA RyhB(60). Similarly, *Salmonella* Typhimurium Bfr is involved in reducing intracellular Fe toxicity, and the absence of Bfr causes increased intracellular free Fe^{2+} ion and oxidative stress(61).

bioRxiv preprint doi: https://doi.org/10.1101/2020.07.15.204859; this version posted May 20, 2021. The copyright holder for this preprint (which was not certified by peer review) is the author/funder, who has granted bioRxiv a license to display the preprint in perpetuity. It is made available under aCC-BY-NC-ND 4.0 International license.

Therefore, we conclude that Δ*yjiY* supernatant treatment inhibits biofilm formation by WT in four major ways- (i) NusG-HNS mediated transcriptional repression of AT-rich SPI-encoded genes, making the WT bacteria less virulent; (ii) FlgM mediated downregulation of class III flagellar genes, impairing flagella-mediated initial attachment to abiotic surfaces, (iii) High abundance of proteases and proteolytic molecules, hindering cell-cell adhesion, and cellular aggregate formation in the EPS matrix, and (iv) Ecotin mediated inhibition of proteases that are necessary during biofilm dispersal. We reasoned that the lower abundance of redox homeostasis proteins and ferritin-like molecules in the Δ*yjiY* supernatant might facilitate the accumulation of toxic oxidative species, causing cellular stress and toxicity. In this light, these oxidative stress relieving proteins can be exploited as potential druggable targets to inhibit *Salmonella* biofilm initiation.

Materials and Methods

Bacterial strains

All *Salmonella* Typhimurium strains used in this study are listed in the following section with their genetic descriptions. *Salmonella enterica* serovar Typhimurium strain 14028S was used as the wild type strain, and was also the parental background for all the mutant strains used in this study, i.e. Δ*yjiY*, Δ*csgD*, Δ*fliC* and Δ*fliC* Δ*fljB*. All strains were grown and maintained in Lennox broth (LB; 0.5% NaCl, 1% casein enzyme hydrolysate and 0.5% yeast extract) at 37˚C under shaking conditions. STM GFP, STM mCherry (RFP-STM-WT) and STM *Δ yjiY:yjiY* were cultured in Lennox broth with 50 µg/ml Ampicillin at 37˚C in shaking condition. *E.coli* DH5α,

bioRxiv preprint doi: https://doi.org/10.1101/2020.07.15.204859; this version posted May 20, 2021. The copyright holder for this preprint (which was not certified by peer review) is the author/funder, who has granted bioRxiv a license to display the preprint in perpetuity. It is made available under aCC-BY-NC-ND 4.0 International license.

338 *Staphylococcus aureus*, *Pseudomonas aeruginosa* and *Klebsiella pneumoniae* were grown in
339 Lennox Broth at 37˚C in shaking condition.

340 List of strains used in this study.

Strain name	**Description**	**Reference**
S. Typhimurium ATCC 14028S (STM_WT)	Wild type (WT)	Kind gift from Prof. M. Hensel (Division of Microbiology, University of Osnabrück, Germany)
Δ*yjiY*	Isogenic knockout strain for the gene *yjiY*; Kan^r	Garai *et al.* (2016)
Δ*csgD*	Isogenic knockout strain for the gene *csgD*; Chl^r	Srinandan *et al.* (2015)
Δ*fliC*	Isogenic knockout strain for the gene *fliC*; Chl^r	Garai *et al.* (2016)
Δ*yjiY*-pQE60-*yjiY*	Isogenic complement strain for Δ*yjiY* expressing *yjiY* under the promoter of T5 present in the plasmid pQE60; Amp^r	Garai *et al.* (2016)
Δ*fliC* Δ*fljB*	Isogenic double knockout strain for *fliC* and *fljB*; Kan^r Chl^r	Karmakar *et al.* (2019)

bioRxiv preprint doi: https://doi.org/10.1101/2020.07.15.204859; this version posted May 20, 2021. The copyright holder for this preprint (which was not certified by peer review) is the author/funder, who has granted bioRxiv a license to display the preprint in perpetuity. It is made available under aCC-BY-NC-ND 4.0 International license.

STM mCherry (RFP-STM-WT)	STM 14028s wildtype strain carrying pFPV-mCherry plasmid, Amp^r	This study
STM GFP	*S.* Typhimurium rpsM promoter driving gfpmut3 expression through pFPV25.1 plasmid, Amp^r	This study

341

342 **Growth conditions for biofilm formation**

343 LB without NaCl, i.e. 1% casein enzyme hydrolysate and 0.5% yeast extract, was used as biofilm
344 media. Overnight cultures grown in LB were subcultured in 2 ml biofilm medium at the dilution
345 of 1:100 in a flat-bottom 24-well polystyrene plate (Tarsons) and incubated at 28˚C for 72 hours
346 without shaking. All images of biofilm in the form of a pellicle were taken with a digital camera
347 (Olympus Stylus VH-520).

348 **Preparation of cell free supernatant**

349 To 2 mL of biofilm media, 1:100 dilution of overnight grown culture was added in flat-bottom
350 24-well polystyrene plate (Tarsons). The plate was incubated at 28˚C without shaking for 72
351 hours. After 72 hours, the media from each well was collected, centrifuged twice at 10000 rpm
352 for 15 minutes, the supernatant was collected and filtered using a 0.2 µm filter and stored at -
353 20˚C. To collect supernatant from M9 (0.5% glucose) media, the cultures were grown at 37˚C in
354 shaking conditions. After 72 hours, the supernatant was collected as described above.

355 **Bacterial biofilm inoculation with culture supernatant**

bioRxiv preprint doi: https://doi.org/10.1101/2020.07.15.204859; this version posted May 20, 2021. The copyright holder for this preprint (which was not certified by peer review) is the author/funder, who has granted bioRxiv a license to display the preprint in perpetuity. It is made available under aCC-BY-NC-ND 4.0 International license.

To test the effect of the 3 day culture supernatant (chemically treated and untreated) on biofilm formation, 20 µl of STM WT overnight culture and indicated volume (1% v/v and/or as indicated in the figures) of the supernatants (WT supernatant, *⊿yjiY* supernatant, Δ*yjiY:yjiY* supernatant and *⊿csgD* supernatant) was added to 2 ml of biofilm media, and incubated under biofilm inducing condition. **Cell pellets** were collected from 3 day old biofilm culture by harvesting the contents of the flat-bottom 24-well polystyrene plates (Tarsons), centrifuging at 10000 rpm for 15 minutes. The cells were resuspended in fresh biofilm inducing media and added at the concentration of $0.5x10^7$ CFU/ml of biofilm media and 20 µl of STM WT overnight culture, and incubated under biofilm inducing condition. For **co-culture** experiments, the overnight cultures of the strains were added in 1:1 ratio to 2 ml of biofilm media and incubated under biofilm inducing condition. **Cell lysates** were prepared by adding 30 µl 1x TME buffer (25 mM Tris pH 8.0, 1 mM EDTA pH 8.0, 2 mM β-mercaptoethanol) and sonicating the bacterial samples (STM WT, STM *⊿yjiY*, and STM Δ*yjiY:yjiY*). The samples were centrifuged at 12000 rpm for 10 minutes and 2 µl supernatant was used for inoculation along with 20 µl STM WT overnight culture and 2 ml of biofilm media and incubated under biofilm inducing condition.

Crystal Violet staining

To quantify the biofilm at the solid-liquid interface, crystal violet (CV) staining was carried out as mentioned in Chandra *et al*(14). Briefly, the protocol followed for biofilm formation was the same as mentioned above. After 72 hours, the media in each well was discarded and the plates were thoroughly washed with RO water to remove all planktonic cells. The plates were then dried and 2 ml of 1% CV was added into each well. After 15 minutes, the CV was removed, and the excessive stain was thoroughly rinsed with RO water. The stained biofilm was destained with 70% ethanol and the intensity of color of the destained solution was quantified at OD_{595} in Tecan

bioRxiv preprint doi: https://doi.org/10.1101/2020.07.15.204859; this version posted May 20, 2021. The copyright holder for this preprint (which was not certified by peer review) is the author/funder, who has granted bioRxiv a license to display the preprint in perpetuity. It is made available under aCC-BY-NC-ND 4.0 International license.

379 plate reader (Infinite Pro 200). The absorbance was plotted in GraphPad Prism 6 and significance
380 values determined using Student's t-test or two-way ANOVA.

381 **Confocal microscopy**

382 Sterile square coverslips (18 mm) were placed in flat-bottom 12-well polystyrene plate
383 (Tarsons). Cultures were inoculated for biofilm formation as mentioned previously. After 72
384 hours, biofilm appeared on the coverslip at the liquid–air interface, in the form of a thin line
385 spanning the width of the coverslip (18 mm). The coverslip was washed thoroughly with water to
386 remove planktonic cells and stained with Congo red (20 mg/ml in water) for 20 min at room
387 temperature. After washing with water, the coverslip was mounted on a slide and imaged for
388 biofilm distribution, with a laser scanning confocal microscope (Zeiss LSM 710) using a 40x
389 objective. Z stacks were taken to generate a three-dimensional image. The MFI of the images
390 were calculated using the ImageJ software. The MFI and thickness of the biofilm were plotted
391 using GraphPad Prism 6. Single layer of cells were imaged and cell length of ~1000 cells from
392 each coverslips was measured using ImageJ.

393 **Glass bead assay**

394 To test the strength of the pellicle at the air-liquid interface, medium sized (0.5mm to 1mm) glass
395 beads were added one by one onto the pellicle. The initial weight of the glass beads was noted,
396 and the number of glass beads added until the pellicle just collapsed was noted down and plotted
397 using GraphPad Prism 6.

398 **Scanning electron microscopy**

399 Biofilm was allowed to form on coverslips as mentioned in the previous section. After thorough
400 washing with water, the sample was fixed in 2.5% gluteraldehyde for 48 hours at room

bioRxiv preprint doi: https://doi.org/10.1101/2020.07.15.204859; this version posted May 20, 2021. The copyright holder for this preprint (which was not certified by peer review) is the author/funder, who has granted bioRxiv a license to display the preprint in perpetuity. It is made available under aCC-BY-NC-ND 4.0 International license.

temperature. Excess gluteraldehyde was removed by washing with water and the sample was dehydrated by gradient washes in increasing concentrations of 30%, 50%, 75%, 85% and 95% ethanol. The coverslips were then air dried under vacuum before coating with gold (JOEL-JFC-1100E ion sputtering device) for imaging by scanning electron microscope. For checking flagellar morphology, 20 µl of STM WT overnight culture and 20 µl of supernatant treated STM WT were smeared on autoclaved 18mm coverslips, air dried, and processed using the abovementioned protocol. Flagellar structure was imaged using field emission-SEM (FEI Sirion, Eindhoven, The Netherlands) scanning electron microscope.

Atomic force microscopy

Sterile 18 mm square coverslips were placed in flat-bottom 12-well polystyrene plates (Tarsons) and biofilm inoculation was done. After 72 hours, the coverslips were removed and washed with sterile MilliQ water. The coverslips were dried and AFM analysis was done using XEISS AFM systems and was analyzed using XEI software.

Supernatant conditioning

The supernatant was treated with different concentrations of EDTA (2.5 mM, 5 mM, 7.5 mM and 10 mM) and incubated at 65˚C for 1 hour. To 200 µl of supernatant, 10 µl of proteinase-K (NEB, stock 20 mg/ml) was added and incubated at 37˚C for 1 hour. The proteinase was inactivated with 0.5 mM PMSF and incubated at 28˚C for 1 hour. The supernatant was heated to 37˚C (60 min), 65˚C (15 min) or 95˚C (15 min) for indicated time and immediately frozen at -20˚C. The pH of the biofilm inducing media as well as that of the supernatant were adjusted using concentrated HCl and 10N NaOH to obtain pH of 4, 7.4, and 9. The supernatants were also

bioRxiv preprint doi: https://doi.org/10.1101/2020.07.15.204859; this version posted May 20, 2021. The copyright holder for this preprint (which was not certified by peer review) is the author/funder, who has granted bioRxiv a license to display the preprint in perpetuity. It is made available under aCC-BY-NC-ND 4.0 International license.

422 treated with 10 µl RNase (stock 1 mg/ml) for 1 hour at 37˚C. Post treatment, the supernatants
423 were used to inoculate biofilm in order to check the activity of the inhibitory molecule(s).

424 **Preformed biofilm disruption**

425 STM WT was allowed to form biofilm as described earlier. 72 hours post inoculation, the formed
426 biofilms were treated with 20, 50 or 100 µl (1% (v/v), 2.5% (v/v) or 5% (v/v), respectively)
427 supernatants and was incubated at 28˚C for 72 hours and biofilm was quantified using CV
428 staining.

429 **Recovery of biofilm formation**

430 STM WT was allowed to form biofilm in the presence of supernatants as described earlier. 72
431 hours post inoculation, the cells were harvested by centrifuging the culture at 10000 rpm for
432 15min. 20 µl of these treated or untreated cells were inoculated in fresh biofilm media (with and
433 without supernatants for retreatment or recovery, respectively) and incubated at 28˚C for 72
434 hours and biofilm was quantified using CV staining.

435 **Supernatant concentrating and separation based on molecular weight**

436 The supernatants from biofilm culture were harvested and filter sterilized as previously
437 mentioned. 4 ml of the supernatants were transferred to the Amicon ultra filter device (Amicon®
438 Ultra-4 centrifugal filter device, 3k MWCO, UFC800324) and centrifuged at 4000g for 30 min in
439 a swing bucket rotor. The concentrated solute from the bottom of the filter device was collected
440 by inserting a pipette.

441 **Quantitative RT PCR**

bioRxiv preprint doi: https://doi.org/10.1101/2020.07.15.204859; this version posted May 20, 2021. The copyright holder for this preprint (which was not certified by peer review) is the author/funder, who has granted bioRxiv a license to display the preprint in perpetuity. It is made available under aCC-BY-NC-ND 4.0 International license.

442 STM WT was allowed to form biofilm in the presence or absence of supernatants as described
443 earlier. After 72 hours, the biofilm population as well as the planktonic cells were harvested by
444 thorough pipetting and centrifugation. From these cells, RNA was isolated by the TRIzol method
445 (Takara). cDNA was synthesized with reverse transcriptase (GCC Biotech). Quantitative PCR
446 was carried out using SYBR Green Q-PCR kit (Takara).

447 List of oligonucleotides used in this study.

Gene	**RT primer sequence (5'-3')**
csgD	FP: ACGATTATCCCTACCGTGAA RP: GCGGACTCGGTGCTGTTGTA
bcsA	FP: CTGCACCAGTCCGTAAAACA RP: AGTTTGTGGCGATCTTCGATT
bapA	FP: ACGGTGACTACGCCTAAAAC RP: CTTCCGCCTCAGTCACTTTT
fliC	FP: CTAAACAAACTGGGTGGCGC RP: GCACCCAGGTCAGAACGTAA
fimA	FP: TTCGGATCGCAGTCATTCAG RP: GTTGCGGCTGATCCTACTC
invF	FP: AGATCGTAAACGCTGCGAGT RP: CTGCTGCACAAACGACGAAA

bioRxiv preprint doi: https://doi.org/10.1101/2020.07.15.204859; this version posted May 20, 2021. The copyright holder for this preprint (which was not certified by peer review) is the author/funder, who has granted bioRxiv a license to display the preprint in perpetuity. It is made available under aCC-BY-NC-ND 4.0 International license.

phoP	FP: GATCTCTCACGCCGGGAATT RP: TGACATCGTGCGGATACTGG
sodA	FP: CCTGCCGGTTGAAGAACTGA RP: GGTTGCTGCTGCTTTTTCGA
ssaV	FP: TATTGATAGGCGCGGACGCTA RP: CGCCTTATGGGCCATGTCTTT
mgtC	FP: GGACCGAACCTAACCCTTG RP: AACTCCCAATATCCGCTGAG
16s rRNA	FP: GTGAGGTAACGGCTCACCAA RP: TAACCGCAACACCTTCCTCC

***In vitro* motility assay**

2 µl of bacterial samples (treated or untreated) were spotted onto the 0.3% agar plates supplemented with 0.5% yeast extract, 1% casein enzyme hydrolysate, 0.5% NaCl and 0.5% glucose (swim agar plates) or 0.5% agar plates supplemented with 0.5% yeast extract, 1% casein enzyme hydrolysate, 0.5% NaCl and 0.5% glucose (swarm agar plates). The plates were incubated at 37˚C and images were taken every 2 hours using a digital camera (Olympus). The diameters of the motility halos were measured using ImageJ. At least five replicate plates were used for each condition, and statistical significance was calculated using Student's *t*-test.

Transmission electron microscope

bioRxiv preprint doi: https://doi.org/10.1101/2020.07.15.204859; this version posted May 20, 2021. The copyright holder for this preprint (which was not certified by peer review) is the author/funder, who has granted bioRxiv a license to display the preprint in perpetuity. It is made available under aCC-BY-NC-ND 4.0 International license.

Flagella and fimbriae were visualised using the protocol described in Garai et al 2016(9). Briefly, overnight STM WT were inoculated with or without supernatants in biofilm media and kept under biofilm inducing condition for 72 hours. After 72 hours, both biofilm and planktonic cells were collected and fixed with 2.5% glutaraldehyde overnight at 4˚C. Similarly fixed overnight cultures of STM WT and STM Δ*fliC* Δ*fljB* were used as positive and negative control, respectively. 2 µl of the cell suspension was added on copper grid, air dried, stained with 1% uranyl acetate for 30 sec, and visualised under transmission electron microscope.

In vitro intracellular survival assay

Int407 cells (ATCC® CCL-6™) were seeded at a density of $2x10^5$ cells per well in flat-bottom 24-well polystyrene plates (Tarsons). 72 hours old supernatant treated or untreated biofilm cultures were sub-cultured, grown to mid-log phase and used for infection of Int407 at MOI 10. The plates were incubated at 37˚C with 5% CO_2 for 20 min to allow infection of the cells. The cells were incubated for an hour in 100 µg/ml Gentamicin. The cells were then washed, and grown in DMEM containing 25 µg/ml Gentamicin. After 1h, 2h and 16h, the cells were lysed with 0.1% Triton-X100 and bacterial load was estimated by plating on SS- agar plates.

In vivo virulence in *C. elegans* N2 worms

STM-RFP bacteria were treated with the supernatants, and kept for biofilm formation for 72 hours. After that, STM-RFP cells were harvested as mentioned before, and 10^7 CFU were seeded on NGM plates, incubated for 12 hours at 37 ^oC. *E. coli* OP50 fed *Caenorhabditis elegans* N2 young adults were harvested in M9 buffer, counted and approximately 150 worms were fed with supernatant treated or untreated 10^7CFU of STM WT RFP bacteria for 12 hours. The worms were then harvested in 1ml M9 buffer, washed 6-8 times to remove extracellular *Salmonella*. 10

bioRxiv preprint doi: https://doi.org/10.1101/2020.07.15.204859; this version posted May 20, 2021. The copyright holder for this preprint (which was not certified by peer review) is the author/funder, who has granted bioRxiv a license to display the preprint in perpetuity. It is made available under aCC-BY-NC-ND 4.0 International license.

480 worms from each sample were transferred to sterile M9 buffer containing 0.5mm sterile glass
481 beads. The worms were lysed, and the gut content of the worms was plated on SS-agar plates.
482 ~20 worms were taken for laser scanning confocal microscopy analysis using Zeiss LSM 880
483 with Multiphoton mode. ~50 worms were transferred to *E. coli* OP50 plate and fed for another
484 12 hours. After 12 hours, the worms were sampled in a similar manner for CFU analysis and
485 imaging.

486 **SDS-PAGE and colloidal Coomassie Blue staining**

487 The proteins in the supernatants were quantified by Bradford's assay and equal quantity of the
488 STM WT and STM Δ*yjiY* supernatants were loaded onto the SDS-PAGE gel (5% stacking, 10%
489 resolving). The gel was then stained with colloidal Coomassie Brilliant Blue R-250 for 3 days
490 and then washed with water to remove excessive stain and visualize the band.

491 **LC QTOF MS/MS analysis of the supernatants**

492 Total protein from the 10-fold concentrated supernatants was subjected to in-solution trypsin
493 digestion for LC Q-TOF MS analysis. Briefly, 200 mg of total protein was resuspended in 200 µl
494 of 50 mM Ammonium bicarbonate. To this, 10 mM DTT was added, and incubated at 56˚C for
495 30 min, followed by alkylation with 20 mM iodoacetamide and incubation at 37˚C for 30 min in
496 dark. For protein digestion, trypsin solution was added to the sample to a final protease to protein
497 ratio of 1:50 (w/w) and incubated at 37˚C for 16 hours, with frequent shaking. The reaction was
498 stopped by adding 10 µl of 0.1% formic acid, and samples were stored at -20˚C until loaded on
499 the Agilent AdvanceBio Peptide Map column (2.1 ×150 mm, 2.7µ). 20 µl of the digested
500 samples were injected to the column, and analysed at a flow rate of 0.4 ml/min using 0.1%
501 formic acid in water as mobile phase A and 0.1% formic acid in acetonitrile as mobile phase B.

bioRxiv preprint doi: https://doi.org/10.1101/2020.07.15.204859; this version posted May 20, 2021. The copyright holder for this preprint (which was not certified by peer review) is the author/funder, who has granted bioRxiv a license to display the preprint in perpetuity. It is made available under aCC-BY-NC-ND 4.0 International license.

All the samples were analyzed using Agilent 1290 Infinity II LC System coupled with Agilent AdvanceBio Q-TOF (6545XT). The MS and MS/MS scan were acquired in the positive mode and stored in centroid mode. The MS data acquisition parameters were as follows- Vcap was set at 3500V, drying gas flow rate and temperature was set at 13 ml/min and 325 ˚C, respectively. A collision energy with a slope of 3.6 V/100 Da and an offset of 4.8 V was used for fragmentation. The Precursor ion data were captured in a mass range of *m/z* 200– 2700 and fragment ions data were acquired between *m/z* 50–2800. The raw data were analyzed using MaxQuant software (v1.6.2.10) and processed through MS excel sheet. The database analysis was performed against *Salmonella* Typhimurium proteome in UniProt (Proteome ID: UP000002695). Following search parameters were used for the database analysis: Precursor mass tolerance: 10ppm, fragment mass tolerance: 40ppm, fixed modifications: carbamidomethyl (C), variable modification: oxidation.

Cloning, expression and purification of ecotin, HNS and NusG

S. Typhimurium 14028S Ecotin (STM14_2792), HNS (STM14_2116) and NusG (STM14_4985) were cloned with 6x His tag in pET15b vector using Gibson assembly. Positive clones were confirmed by PCR and transformed in *E. coli* BL21 (DE3) pLysS strain. *E. coli* BL21 (DE3) cells bearing expression plasmids were grown overnight at 37°C in LB media containing 50 µg/ml chloramphenicol and 100 µg/ml ampicillin. 1% of the primary inoculum was added to 500ml of LB media containing 100 µg/ml ampicillin and grown at 37°C till the culture attained an OD_{600} of ~ 0.8, and induced with 1mM isopropyl β-D-1-thiogalactopyranoside (IPTG) at 30°C for 6 hours. The cells were harvested by centrifugation, and the pellet was resuspended in 20ml ice-cold resuspension buffer (0.2M Tris (pH 7.5), 0.5mM EDTA, and 1mM PMSF). Further, the cells were lysed by sonication on ice, followed by centrifugation at 14000g. The protein was purified from the soluble fraction of the lysate by affinity chromatography using Ni-

bioRxiv preprint doi: https://doi.org/10.1101/2020.07.15.204859; this version posted May 20, 2021. The copyright holder for this preprint (which was not certified by peer review) is the author/funder, who has granted bioRxiv a license to display the preprint in perpetuity. It is made available under aCC-BY-NC-ND 4.0 International license.

525 NTA column. Protein was eluted with linear gradient of 0.1-1M imidazole in 50mM Tris (pH
526 8.0). Elute fractions containing protein of interest were pooled, concentrated and subjected to
527 purification by size exclusion chromatography (SEC) on Superdex 75 Increase 10/300GL
528 column (with a flow rate of 0.5 ml/min and 500 µl sample injection volume) equilibrated with
529 50mM Tris (pH 8.0). The peaks obtained from the chromatogram were analyzed by subjecting
530 the collected fractions (which were pooled and concentrated after SEC) to SDS-PAGE, to obtain
531 the protein of interest in its desired monomeric form. The protein purity was also confirmed by
532 MALDI-TOF.

533 List of oligonucleotides used for cloning.

Oligo Name	Primer sequences (5'-3')
pET15b_Ecotin	**FP:**CGGCCTGGTGCCGCGCGGCAGCCATATGAAGAT GTTTGTCCCTGCCG
	RP:CTTTCGGGCTTTGTTAGCAGCCGGATCCTCATCG CGCGACGGCGTTC
pET15b_HNS	**FP:**GCGGCCTGGTGCCGCGCGGCAGCCATATGAGCG AAGCACTTAAAATTC
	RP:TTTCGGGCTTTGTTAGCAGCCGGATCCTTATTCC TTGATCAGGAAATCTTCC
pET15b_NusG	**FP:**AGCGGCCTGGTGCCGCGCGGCAGCCATATGTCTG AAGCACCTAAAAAGC
	RP:TCGGGCTTTGTTAGCAGCCGGATCCTTACGCTTT CTCAACCTGACTG

534

bioRxiv preprint doi: https://doi.org/10.1101/2020.07.15.204859; this version posted May 20, 2021. The copyright holder for this preprint (which was not certified by peer review) is the author/funder, who has granted bioRxiv a license to display the preprint in perpetuity. It is made available under aCC-BY-NC-ND 4.0 International license.

Statistical analysis

Statistical analyses were performed with GraphPad Prism software. Student's t test and one-way or two-way ANOVA tests were performed as indicated. The results are expressed as mean ± SD or mean ± SEM. Group sizes, experiment number, and p values for each experiment are described in the figure legends.

Acknowledgements

We thank the electron microscopy facility of IISc, AFMM facility of IISc, Atomic force microscopy facility of BSSE, IISc and confocal microscopy facility and real-time facility of Dept. of Microbiology and Cell Biology, IISc. We thank Mr. Priyabrata (TH lab, MRDG, IISc) for the helping with the TEM sample preparation. We thank Dr Shahbaz and Dr Jayantika (RV lab, MBU, IISc) for helping with cloning, protein expression and purification. We are very grateful to Dr Kapudeep and Ms. Meghanashree for their valuable inputs.

Funding

This work was supported by the DAE SRC fellowship (DAE00195) and DBT-IISc partnership umbrella program for advanced research in BioSystems Science and Engineering to DC. Infrastructure support from ICMR (Centre for Advanced Study in Molecular Medicine), DST (FIST), and UGC (special assistance) is acknowledged.

Author Contribution

KC and DC conceived the study and designed experiments. KC and PM performed experiments. SK performed and UST provided valuable inputs for the LC QTOF MS/MS experiment. KC analyzed the data, prepared the figures and wrote the manuscript. DC supervised the work. All the authors read and approved the manuscript.

bioRxiv preprint doi: https://doi.org/10.1101/2020.07.15.204859; this version posted May 20, 2021. The copyright holder for this preprint (which was not certified by peer review) is the author/funder, who has granted bioRxiv a license to display the preprint in perpetuity. It is made available under aCC-BY-NC-ND 4.0 International license.

Competing Interests

The authors declare no competing interests.

References

1. Bakhshi B, Dehghan-Mouriaabadi A, Kiani P. 2018. Heterogeneity of Multidrug-Resistant Salmonella enterica Isolates with Increasing Frequency of Resistance to Ciprofloxacin During a 4-Year Period in Iran. Microb Drug Resist 24:479-488.
2. Michael GB, Schwarz S. 2016. Antimicrobial resistance in zoonotic nontyphoidal Salmonella: an alarming trend? Clin Microbiol Infect 22:968-974.
3. WHO. 2018. Salmonella (non -typhoidal) Fact sheet. https://www.who.int/en/news-room/fact-sheets/detail/salmonella-(non-typhoidal). Accessed
4. Krzysciak P, Chmielarczyk A, Pobiega M, Romaniszyn D, Wojkowska-Mach J. 2017. Acinetobacter baumannii isolated from hospital-acquired infection: biofilm production and drug susceptibility. APMIS 125:1017-1026.
5. Di Lodovico S, Cataldi V, Di Campli E, Ancarani E, Cellini L, Di Giulio M. 2017. Enterococcus hirae biofilm formation on hospital material surfaces and effect of new biocides. Environ Health Prev Med 22:63.
6. Di Domenico EG, Cavallo I, Pontone M, Toma L, Ensoli F. 2017. Biofilm Producing Salmonella Typhi: Chronic Colonization and Development of Gallbladder Cancer. Int J Mol Sci 18.
7. Prouty AM, Schwesinger WH, Gunn JS. 2002. Biofilm formation and interaction with the surfaces of gallstones by Salmonella spp. Infect Immun 70:2640-9.
8. Grantcharova N, Peters V, Monteiro C, Zakikhany K, Romling U. 2010. Bistable expression of CsgD in biofilm development of Salmonella enterica serovar typhimurium. J Bacteriol 192:456-66.

bioRxiv preprint doi: https://doi.org/10.1101/2020.07.15.204859; this version posted May 20, 2021. The copyright holder for this preprint (which was not certified by peer review) is the author/funder, who has granted bioRxiv a license to display the preprint in perpetuity. It is made available under aCC-BY-NC-ND 4.0 International license.

9. Garai P, Lahiri A, Ghosh D, Chatterjee J, Chakravortty D. 2016. Peptide utilizing carbon starvation gene yjiY is required for flagella mediated infection caused by Salmonella. Microbiology 162:100-116.

10. Khil PP, Camerini-Otero RD. 2002. Over 1000 genes are involved in the DNA damage response of Escherichia coli. Mol Microbiol 44:89-105.

11. Soufi B, Krug K, Harst A, Macek B. 2015. Characterization of the E. coli proteome and its modifications during growth and ethanol stress. Front Microbiol 6:103.

12. Goswami M, Narayana Rao A. 2018. Transcriptome Profiling Reveals Interplay of Multifaceted Stress Response in Escherichia coli on Exposure to Glutathione and Ciprofloxacin. mSystems 3.

13. Garai P, Chandra K, Chakravortty D. 2017. Bacterial peptide transporters: Messengers of nutrition to virulence. Virulence 8:297-309.

14. Chandra K, Garai P, Chatterjee J, Chakravortty D. 2017. Peptide transporter YjiY influences the expression of the virulence gene mgtC to regulate biofilm formation in Salmonella. FEMS Microbiol Lett 364.

15. Iwase T, Uehara Y, Shinji H, Tajima A, Seo H, Takada K, Agata T, Mizunoe Y. 2010. Staphylococcus epidermidis Esp inhibits Staphylococcus aureus biofilm formation and nasal colonization. Nature 465:346-9.

16. Fang K, Jin X, Hong SH. 2018. Probiotic Escherichia coli inhibits biofilm formation of pathogenic E. coli via extracellular activity of DegP. Sci Rep 8:4939.

17. Hong SH, Hegde M, Kim J, Wang X, Jayaraman A, Wood TK. 2012. Synthetic quorum-sensing circuit to control consortial biofilm formation and dispersal in a microfluidic device. Nat Commun 3:613.

18. Lee J, Jayaraman A, Wood TK. 2007. Indole is an inter-species biofilm signal mediated by SdiA. BMC Microbiol 7:42.

bioRxiv preprint doi: https://doi.org/10.1101/2020.07.15.204859; this version posted May 20, 2021. The copyright holder for this preprint (which was not certified by peer review) is the author/funder, who has granted bioRxiv a license to display the preprint in perpetuity. It is made available under aCC-BY-NC-ND 4.0 International license.

19. Jayaraman A, Hallock PJ, Carson RM, Lee CC, Mansfeld FB, Wood TK. 1999. Inhibiting sulfate-reducing bacteria in biofilms on steel with antimicrobial peptides generated in situ. Appl Microbiol Biotechnol 52:267-75.

20. Mowat E, Rajendran R, Williams C, McCulloch E, Jones B, Lang S, Ramage G. 2010. Pseudomonas aeruginosa and their small diffusible extracellular molecules inhibit Aspergillus fumigatus biofilm formation. FEMS Microbiol Lett 313:96-102.

21. Gnanadhas DP, Elango M, Janardhanraj S, Srinandan CS, Datey A, Strugnell RA, Gopalan J, Chakravortty D. 2015. Successful treatment of biofilm infections using shock waves combined with antibiotic therapy. Sci Rep 5:17440.

22. Datey A, Thaha CSA, Patil SR, Gopalan J, Chakravortty D. 2019. Shockwave Therapy Efficiently Cures Multispecies Chronic Periodontitis in a Humanized Rat Model. Front Bioeng Biotechnol 7:382.

23. Steenackers H, Hermans K, Vanderleyden J, Sigrid CJ, Keersmaecker D. 2012. Salmonella biofilms: An overview on occurrence, structure, regulation and eradication. Food Res Int 45:502-531.

24. Yuksel FN, Buzrul S, Akcelik M, Akcelik N. 2018. Inhibition and eradication of Salmonella Typhimurium biofilm using P22 bacteriophage, EDTA and nisin. Biofouling 34:1046-1054.

25. Todorov SD, de Paula OAL, Camargo AC, Lopes DA, Nero LA. 2018. Combined effect of bacteriocin produced by Lactobacillus plantarum ST8SH and vancomycin, propolis or EDTA for controlling biofilm development by Listeria monocytogenes. Rev Argent Microbiol 50:48-55.

26. Gockerman A, Clemmons DR. 1995. Porcine aortic smooth muscle cells secrete a serine protease for insulin-like growth factor binding protein-2. Circ Res 76:514-21.

bioRxiv preprint doi: https://doi.org/10.1101/2020.07.15.204859; this version posted May 20, 2021. The copyright holder for this preprint (which was not certified by peer review) is the author/funder, who has granted bioRxiv a license to display the preprint in perpetuity. It is made available under aCC-BY-NC-ND 4.0 International license.

626 27. Bahgat M, Doenhoff M, Kirschfink M, Ruppel A. 2002. Serine protease and phenoloxidase
627 activities in hemocytes of Biomphalaria glabrata snails with varying susceptibility to infection
628 with the parasite Schistosoma mansoni. Parasitol Res 88:489-94.
629 28. Papenfort K, Forstner KU, Cong JP, Sharma CM, Bassler BL. 2015. Differential RNA-seq of Vibrio
630 cholerae identifies the VqmR small RNA as a regulator of biofilm formation. Proc Natl Acad Sci U
631 S A 112:E766-75.
632 29. Janssen KH, Diaz MR, Gode CJ, Wolfgang MC, Yahr TL. 2018. RsmV, a Small Noncoding
633 Regulatory RNA in Pseudomonas aeruginosa That Sequesters RsmA and RsmF from Target
634 mRNAs. J Bacteriol 200.
635 30. Coughlan LM, Cotter PD, Hill C, Alvarez-Ordonez A. 2016. New Weapons to Fight Old Enemies:
636 Novel Strategies for the (Bio)control of Bacterial Biofilms in the Food Industry. Front Microbiol
637 7:1641.
638 31. O'Toole GA, Kolter R. 1998. Flagellar and twitching motility are necessary for Pseudomonas
639 aeruginosa biofilm development. Mol Microbiol 30:295-304.
640 32. Ammendola S, D'Amico Y, Chirullo B, Drumo R, Ciavardelli D, Pasquali P, Battistoni A. 2016. Zinc
641 is required to ensure the expression of flagella and the ability to form biofilms in Salmonella
642 enterica sv Typhimurium. Metallomics 8:1131-1140.
643 33. Haraga A, Ohlson MB, Miller SI. 2008. Salmonellae interplay with host cells. Nat Rev Microbiol
644 6:53-66.
645 34. Lou L, Zhang P, Piao R, Wang Y. 2019. Salmonella Pathogenicity Island 1 (SPI-1) and Its Complex
646 Regulatory Network. Front Cell Infect Microbiol 9:270.
647 35. Fux CA, Costerton JW, Stewart PS, Stoodley P. 2005. Survival strategies of infectious biofilms.
648 Trends Microbiol 13:34-40.

bioRxiv preprint doi: https://doi.org/10.1101/2020.07.15.204859; this version posted May 20, 2021. The copyright holder for this preprint (which was not certified by peer review) is the author/funder, who has granted bioRxiv a license to display the preprint in perpetuity. It is made available under aCC-BY-NC-ND 4.0 International license.

649 36. Fabrega A, Vila J. 2013. Salmonella enterica serovar Typhimurium skills to succeed in the host:
650 virulence and regulation. Clin Microbiol Rev 26:308-41.
651 37. Chen H, Fang Q, Tu Q, Liu C, Yin J, Yin Y, Xia L, Bian X, Zhang Y. 2018. Identification of a contact-
652 dependent growth inhibition system in the probiotic Escherichia coli Nissle 1917. FEMS
653 Microbiol Lett 365.
654 38. Simm R, Ahmad I, Rhen M, Le Guyon S, Romling U. 2014. Regulation of biofilm formation in
655 Salmonella enterica serovar Typhimurium. Future Microbiol 9:1261-82.
656 39. Desai SK, Padmanabhan A, Harshe S, Zaidel-Bar R, Kenney LJ. 2019. Salmonella biofilms program
657 innate immunity for persistence in Caenorhabditis elegans. Proc Natl Acad Sci U S A 116:12462-
658 12467.
659 40. Ochman H, Groisman EA. 1994. The origin and evolution of species differences in Escherichia coli
660 and Salmonella typhimurium. EXS 69:479-93.
661 41. Chattopadhyay S, Paul S, Kisiela DI, Linardopoulou EV, Sokurenko EV. 2012. Convergent
662 molecular evolution of genomic cores in Salmonella enterica and Escherichia coli. J Bacteriol
663 194:5002-11.
664 42. Meysman P, Sanchez-Rodriguez A, Fu Q, Marchal K, Engelen K. 2013. Expression divergence
665 between Escherichia coli and Salmonella enterica serovar Typhimurium reflects their lifestyles.
666 Mol Biol Evol 30:1302-14.
667 43. Subramaniam S, Muller VS, Hering NA, Mollenkopf H, Becker D, Heroven AK, Dersch P,
668 Pohlmann A, Tedin K, Porwollik S, McClelland M, Meyer TF, Hunke S. 2019. Contribution of the
669 Cpx envelope stress system to metabolism and virulence regulation in Salmonella enterica
670 serovar Typhimurium. PLoS One 14:e0211584.

bioRxiv preprint doi: https://doi.org/10.1101/2020.07.15.204859; this version posted May 20, 2021. The copyright holder for this preprint (which was not certified by peer review) is the author/funder, who has granted bioRxiv a license to display the preprint in perpetuity. It is made available under aCC-BY-NC-ND 4.0 International license.

671 44. Saito T, Ueno T, Kubori T, Yamaguchi S, Iino T, Aizawa SI. 1998. Flagellar filament elongation can
672 be impaired by mutations in the hook protein FlgE of Salmonella typhimurium: a possible role of
673 the hook as a passage for the anti-sigma factor FlgM. Mol Microbiol 27:1129-39.
674 45. Chadsey MS, Karlinsey JE, Hughes KT. 1998. The flagellar anti-sigma factor FlgM actively
675 dissociates Salmonella typhimurium sigma28 RNA polymerase holoenzyme. Genes Dev 12:3123-
676 36.
677 46. Liang H, Li L, Dong Z, Surette MG, Duan K. 2008. The YebC family protein PA0964 negatively
678 regulates the Pseudomonas aeruginosa quinolone signal system and pyocyanin production. J
679 Bacteriol 190:6217-27.
680 47. Bossi L, Ratel M, Laurent C, Kerboriou P, Camilli A, Eveno E, Boudvillain M, Figueroa-Bossi N.
681 2019. NusG prevents transcriptional invasion of H-NS-silenced genes. PLoS Genet 15:e1008425.
682 48. Dorman CJ. 2007. H-NS, the genome sentinel. Nat Rev Microbiol 5:157-61.
683 49. Free A, Dorman CJ. 1995. Coupling of Escherichia coli hns mRNA levels to DNA synthesis by
684 autoregulation: implications for growth phase control. Mol Microbiol 18:101-13.
685 50. Kobayashi H, Miyamoto T, Hashimoto Y, Kiriki M, Motomatsu A, Honjoh K, Iio M. 2005.
686 Identification of factors involved in recovery of heat-injured Salmonella Enteritidis. J Food Prot
687 68:932-41.
688 51. Gur E, Biran D, Shechter N, Genevaux P, Georgopoulos C, Ron EZ. 2004. The Escherichia coli DjlA
689 and CbpA proteins can substitute for DnaJ in DnaK-mediated protein disaggregation. J Bacteriol
690 186:7236-42.
691 52. Doyle SM, Shastry S, Kravats AN, Shih YH, Miot M, Hoskins JR, Stan G, Wickner S. 2015. Interplay
692 between E. coli DnaK, ClpB and GrpE during protein disaggregation. J Mol Biol 427:312-27.

bioRxiv preprint doi: https://doi.org/10.1101/2020.07.15.204859; this version posted May 20, 2021. The copyright holder for this preprint (which was not certified by peer review) is the author/funder, who has granted bioRxiv a license to display the preprint in perpetuity. It is made available under aCC-BY-NC-ND 4.0 International license.

693 53. del Solar GH, de al Campa AG, Perez-Martin J, Choli T, Espinosa M. 1989. Purification and
694 characterization of RepA, a protein involved in the copy number control of plasmid pLS1. Nucleic
695 Acids Res 17:2405-20.
696 54. Kaplan JB. 2010. Biofilm dispersal: mechanisms, clinical implications, and potential therapeutic
697 uses. J Dent Res 89:205-18.
698 55. Henderson B, Martin A. 2011. Bacterial virulence in the moonlight: multitasking bacterial
699 moonlighting proteins are virulence determinants in infectious disease. Infect Immun 79:3476-
700 91.
701 56. Kim YH, Lee Y, Kim S, Yeom J, Yeom S, Seok Kim B, Oh S, Park S, Jeon CO, Park W. 2006. The role
702 of periplasmic antioxidant enzymes (superoxide dismutase and thiol peroxidase) of the Shiga
703 toxin-producing Escherichia coli O157:H7 in the formation of biofilms. Proteomics 6:6181-93.
704 57. La Carbona S, Sauvageot N, Giard JC, Benachour A, Posteraro B, Auffray Y, Sanguinetti M, Hartke
705 A. 2007. Comparative study of the physiological roles of three peroxidases (NADH peroxidase,
706 Alkyl hydroperoxide reductase and Thiol peroxidase) in oxidative stress response, survival inside
707 macrophages and virulence of Enterococcus faecalis. Mol Microbiol 66:1148-63.
708 58. Wu Y, Outten FW. 2009. IscR controls iron-dependent biofilm formation in Escherichia coli by
709 regulating type I fimbria expression. J Bacteriol 191:1248-57.
710 59. Kang D, Kirienko NV. 2018. Interdependence between iron acquisition and biofilm formation in
711 Pseudomonas aeruginosa. J Microbiol 56:449-457.
712 60. Masse E, Gottesman S. 2002. A small RNA regulates the expression of genes involved in iron
713 metabolism in Escherichia coli. Proc Natl Acad Sci U S A 99:4620-5.
714 61. Velayudhan J, Castor M, Richardson A, Main-Hester KL, Fang FC. 2007. The role of ferritins in the
715 physiology of Salmonella enterica sv. Typhimurium: a unique role for ferritin B in iron-sulphur
716 cluster repair and virulence. Mol Microbiol 63:1495-507.

bioRxiv preprint doi: https://doi.org/10.1101/2020.07.15.204859; this version posted May 20, 2021. The copyright holder for this preprint (which was not certified by peer review) is the author/funder, who has granted bioRxiv a license to display the preprint in perpetuity. It is made available under aCC-BY-NC-ND 4.0 International license.

Figure Legends

Fig 1. *Salmonella* biofilm deficient Δ*yjiY* inhibits biofilm formation by WT strain

A. Biofilm formation ability of the WT strain after 72 hours of inoculation in presence or absence of WT, Δ*yjiY,* Δ*yjiY:yjiY* and Δ*csgD* culture supernatants was checked. Crystal violet staining was carried out to check the biofilm formed on the solid-liquid interphase (Data are presented as mean ± SEM of 12 independent experiments). B. Similarly biofilm formation assay was carried out in presence or absence of overnight grown different bacterial strains (co-culture), washed bacterial pellet (cell pellet), cell free supernatant (culture supernatant) and cell lysates (Data are presented as mean ± SEM of 4 independent experiments). C. Different concentration of the cell free supernatant was used to check the minimum biofilm inhibitory concentration (MBIC) of Δ*yjiY* supernatant (Data are presented as mean ± SEM of 4 independent experiments). D. Biofilm inhibitory property of the Δ*yjiY* supernatant was checked with supernatant isolated from bacteria grown in shaking condition in LB media and minimal M9 media (Data are presented as mean ± SEM of 4 independent experiments). Student's t-test was used to analyze the data; p values ****<0.0001, ***<0.001, **<0.01, *<0.05.

Fig 2. *Salmonella Δ*yjiY* cell free supernatant significantly reduces the biofilm biomass by reducing cell-cell adhesion

A. Representative images of biofilm formed on coverslips that were stained with Congo red and imaged using a confocal microscope to generate 3D images and quantify cellulose biomass. Scale is shown on the X- and Y-axes. B. The tensile strength of the biofilm was measured by glass bead assay. Weight of glass beads required to just sink the biofilm to bottom, was plotted

bioRxiv preprint doi: https://doi.org/10.1101/2020.07.15.204859; this version posted May 20, 2021. The copyright holder for this preprint (which was not certified by peer review) is the author/funder, who has granted bioRxiv a license to display the preprint in perpetuity. It is made available under aCC-BY-NC-ND 4.0 International license.

(Data are presented as mean ± SEM of 5 independent experiments). C. Representative scanning electron micrograph of biofilm formed on a coverslip. Scale bar is 10 µm. D. Cell length of the biofilm inoculated treated or untreated STM WT cells was measured using ImageJ, and plotted (Data are presented as mean ± SEM of 1200 cells were measured from 3 independent experiments). E. Representative confocal images of biofilm cells showing a difference in cell length. Scale bar is 5 µm (1000-1200 cells were measured from 3 independent experiments for each treatment). Student's t-test was used to analyze the data; p values ****<0.0001, ***<0.001, **<0.01, *<0.05.

Fig 3. The physicochemical property of the inhibitory molecules is proteinaceous

A. The cell-free supernatants were treated with different concentrations of EDTA and checked for their ability to inhibit biofilm formation by STM WT (Data are presented as mean ± SEM of 3 independent experiments). B. The supernatants were treated with proteinase K, and heated to 37 ˚C for 1 hour, and checked for the biofilm inhibitory activity. PMSF was used to inactivate proteinase K after 1 hour, and was also used as a control (Data are presented as mean ± SEM of 3 independent experiments). C. The supernatants were heated to 65 ˚C and 95 ˚C to check the thermostability of the active component(s), followed by biofilm inoculation with the treated or untreated supernatants (Data are presented as mean ± SEM of 3 independent experiments). D. The pH sensitivity of biofilm inhibitory action of the supernatants were checked. The pH of the supernatants as well as the biofilm media was made acidic (pH 4.0) or alkaline (pH 9.0) with concentrated HCl or NaOH, respectively, and checked for the activity of the active molecule(s) (Data are presented as mean ± SEM of 3 independent experiments). Two-way ANOVA and Student's t-test were used to analyze the data; p values ****<0.0001, ***<0.001, **<0.01, *<0.05.

bioRxiv preprint doi: https://doi.org/10.1101/2020.07.15.204859; this version posted May 20, 2021. The copyright holder for this preprint (which was not certified by peer review) is the author/funder, who has granted bioRxiv a license to display the preprint in perpetuity. It is made available under aCC-BY-NC-ND 4.0 International license.

Fig 4. The supernatant interrupts biofilm formation by transcriptional switching during initiation of micro-colony formation

A. Varied concentrations of the STM Δ*yjiY* supernatant were used to pre-formed mature biofilm of STM WT and the ability of the supernatant to disintegrate the biofilm was checked (Data are presented as mean ± SEM of 5 independent experiments). B. The extent of inhibitory effect of the supernatants were checked by recovery and repeated exposure of the WT strain to the supernatant (Data are presented as mean ± SEM of 3 independent experiments). C. RNA was isolated from untreated STM WT cells or WT cells treated with the indicated supernatants for 72 hours. RTPCR was done for indicated genes, and C_T values were first normalized to 16s rRNA gene and then normalized to that of untreated WT cells. Y axis values above and below 1 denotes upregulation and downregulation, respectively (Data are presented as mean ± SEM of 3 independent experiments). (D, E). *In vitro* motility of the treated and untreated STM WT cells were checked on 0.3% swim agar plates or 0.5% swarm agar plates. The radius of the motile zone was imaged after different time, measured using ImageJ and plotted (Data are presented as mean ± SEM of 4 independent experiments). F. The flagellar status of the treated or untreated cells (approximately 50 cells in each samples, in two different experiments) was imaged using scanning electron microscope. White arrows show the flagella. Scale bar is 500 nm. Two-way ANOVA and Student's t-test were used to analyze the data; p values ****<0.0001, ***<0.001, **<0.01, *<0.05.

Fig 5. STM Δ*yjiY* supernatant treatment impairs virulence of STM WT

A. *In vitro* invasiveness of the supernatant treated WT bacteria was checked by infecting adherent human epithelial Int407 cell line and percent invasion was plotted. Log phase WT culture was used as a control (Data are presented as mean ± SEM of 3 independent experiments).

bioRxiv preprint doi: https://doi.org/10.1101/2020.07.15.204859; this version posted May 20, 2021. The copyright holder for this preprint (which was not certified by peer review) is the author/funder, who has granted bioRxiv a license to display the preprint in perpetuity. It is made available under aCC-BY-NC-ND 4.0 International license.

B. Survival of intracellular *Salmonella* in Int407 cells was checked by gentamicin protection assay. The intracellular bacterial fold proliferation was measured as the ratio of intracellular bacterial CFU after 16 hours to the CFU at 2 hours (Data are presented as mean ± SEM of 3 independent experiments). C. Percent gut colonization was measured by measuring the diameters of the colonized gut and total body width after feeding the worms continuously for 12 hours with mCherry-*E.coli* OP50 or supernatant treated/untreated mCherry-STM WT (approximately total 25 worms were measured in 2 independent experiments). D. Representative images of 3 days supernatant treated bacterial colonization in young adult *C. elegans* N2 worms. Bacterial colonization in the gut lumen was checked after 12 hours of continuous STM WT feeding and/or 12 hours STM WT feeding, followed by 12 hours *E. coli* OP50 feeding (approximately total 25 worms were imaged in 2 independent experiments). Scale bar is 20 µm. E. Bacterial CFU from infected *C. elegans* was determined by lysing 10 worms (in triplicates) in M9 buffer followed by dilution plating (Data are presented as mean ± SEM of 2 independent experiments). Student's t-test was used to analyze the data; p value *<0.05. F. Biofilm inhibitory effect of STM Δ*yjiY* supernatant on few other enterobacteriaceae pathogens was checked by inoculation the strains with 1% v/v supernatants (Ec- *Escherichia coli* DH5α, Pa01- *Pseudomonas aeruginosa* strain PA01, Kpn- *Klebsiella pneumoniae*, Sa- *Staphylococcus aureus*, Data are presented as mean ± -SEM of 3 independent experiments). Two-way ANOVA and Student's t-test were used to analyze the data; p values ****<0.0001, ***<0.001, **<0.01, *<0.05.

Fig 6. Global transcriptional regulator HNS along with NusG causes major transcriptional regulation leading to biofilm inhibition and motility inhibition

A. SDS PAGE of the STM WT and STM Δ*yjiY* supernatant showing presence of multiple differential bands in the supernatants. B. Venn diagram showing proteins present in the

bioRxiv preprint doi: https://doi.org/10.1101/2020.07.15.204859; this version posted May 20, 2021. The copyright holder for this preprint (which was not certified by peer review) is the author/funder, who has granted bioRxiv a license to display the preprint in perpetuity. It is made available under aCC-BY-NC-ND 4.0 International license.

supernatants detected in LC QTOF MS/MS analysis, blue and red circles represent number of proteins found in STM WT and Δ*yjiY* culture supernatants, respectively. C. Biofilm formation ability of the WT strain after 72 hours of inoculation in presence of Δ*yjiY* culture supernatant and 200ng ecotin/HNS/NusG fractions was checked. Crystal violet staining was carried out to check the biofilm formed on the solid-liquid interphase (Data are presented as mean ± SEM of 3 independent experiments; One-way was used to analyze the data; p values ****<0.0001, ***<0.001). D. Proposed model of biofilm inhibition by Δ*yjiY* supernatant. The model depicts that transcription factors, proteases, QS-quenching molecules, and protease inhibitors are secreted actively or released during cell lysis in Δ*yjiY* supernatant, which upon entering into the WT cells by either active transport or membrane diffusion, regulates biofilm formation and motility.

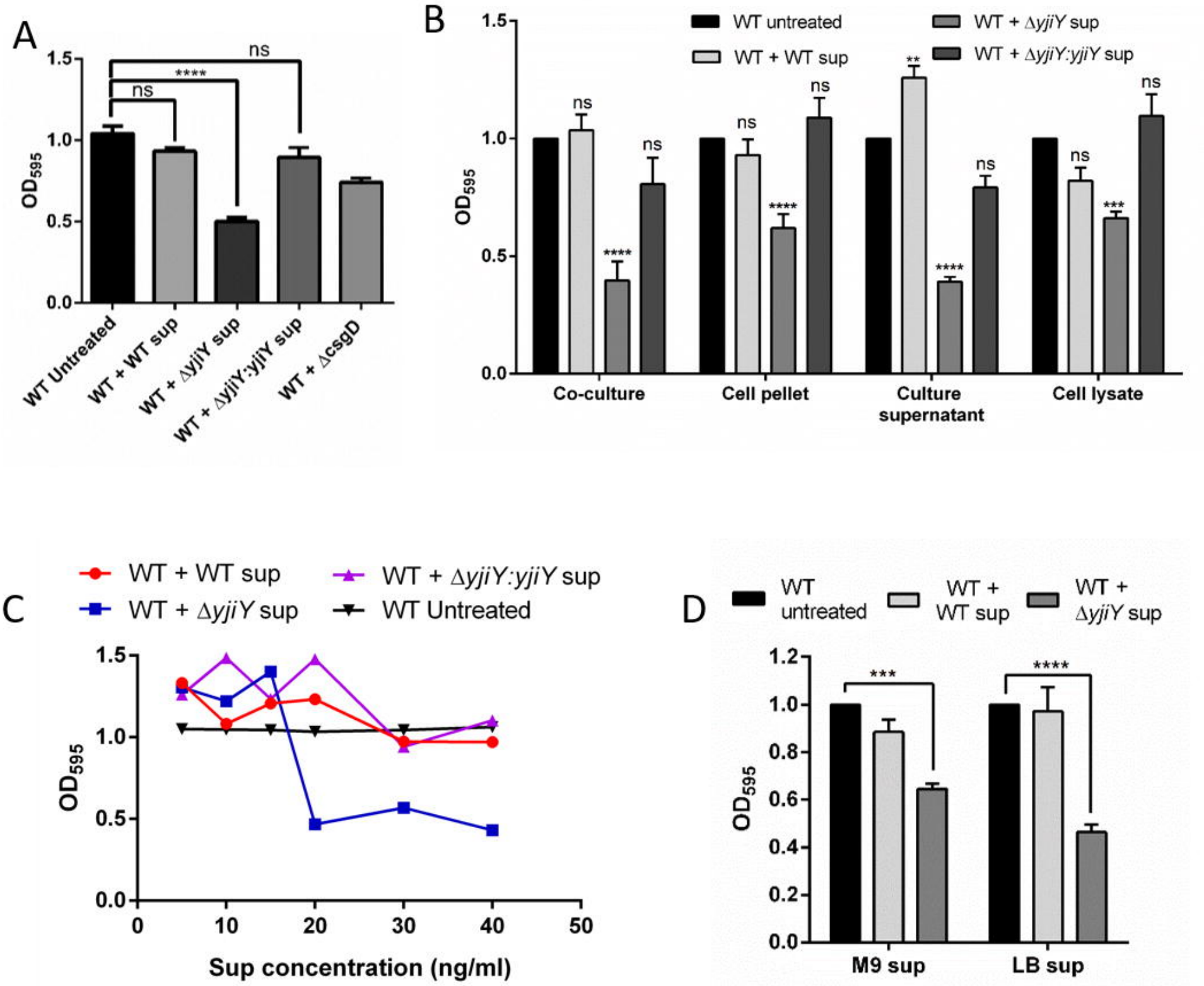
A
B
C
D
WT Untreated
WT + WT sup
WT + ΔyjiY sup
WT + ΔyjiY:yjiY sup
WT + ΔcsgD
OD595
ns
****
**
***
Co-culture
Cell pellet
Culture supernatant
Cell lysate
Sup concentration (ng/ml)
M9 sup
LB sup

A

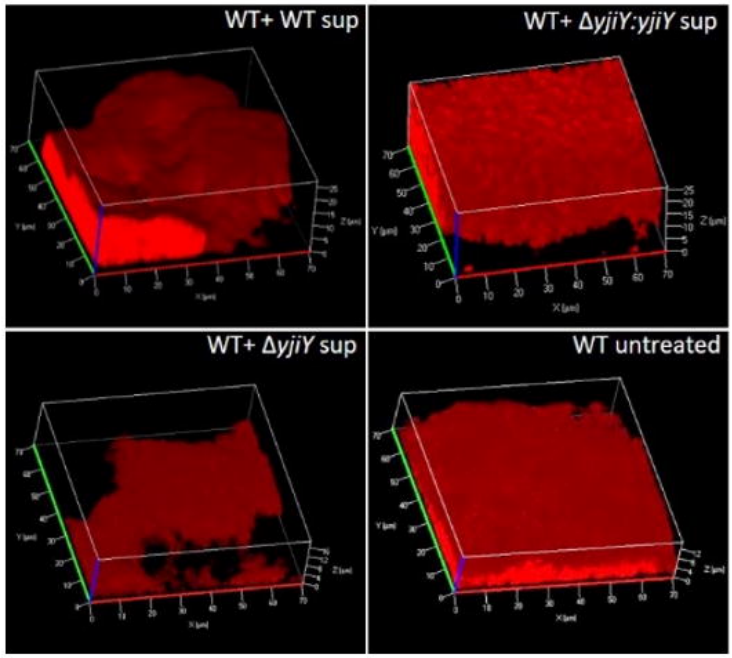
WT+ WT sup
WT+ ΔyjiY:yjiY sup
WT+ ΔyjiY sup
WT untreated

B

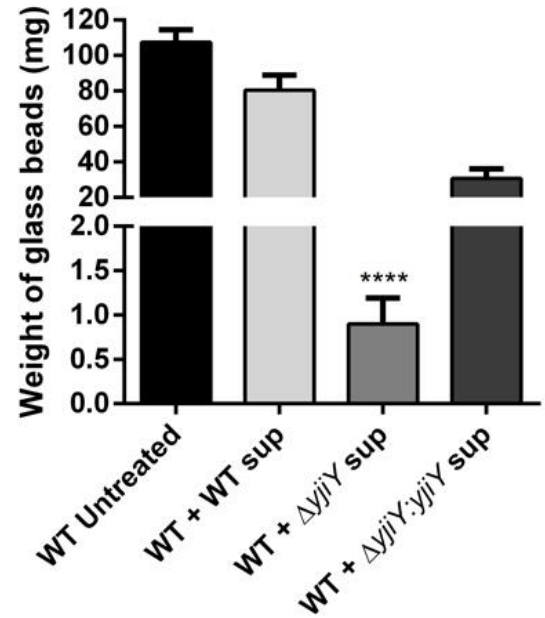
Weight of glass beads (mg)
120
100
80
60
40
20
2.0
1.5
1.0
0.5
0.0
****
WT Untreated
WT + WT sup
WT + ΔyjiY sup
WT + ΔyjiY:yjiY sup

C

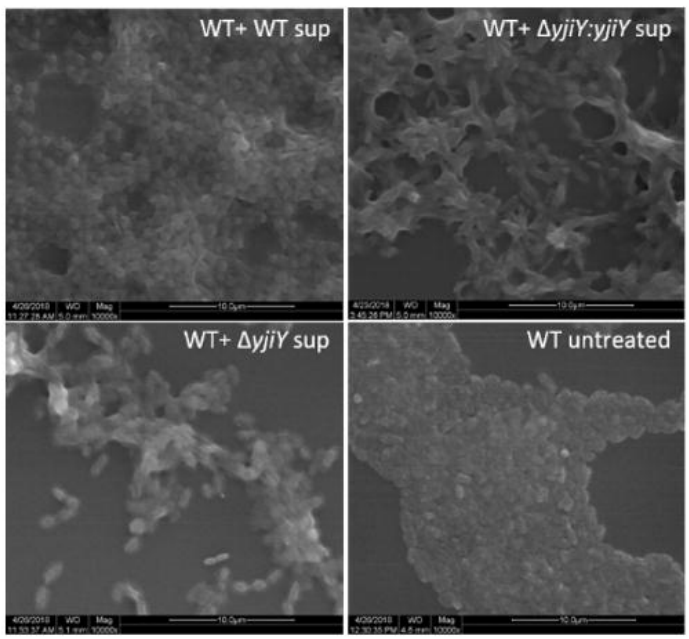
WT+ WT sup
WT+ ΔyjiY:yjiY sup
WT+ ΔyjiY sup
WT untreated

D

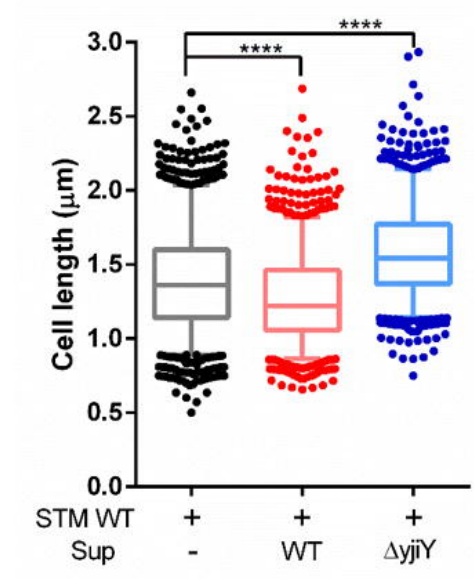
Cell length (μm)
3.0
2.5
2.0
1.5
1.0
0.5
0.0
****
****
STM WT + + +
Sup - WT ΔyjiY

E

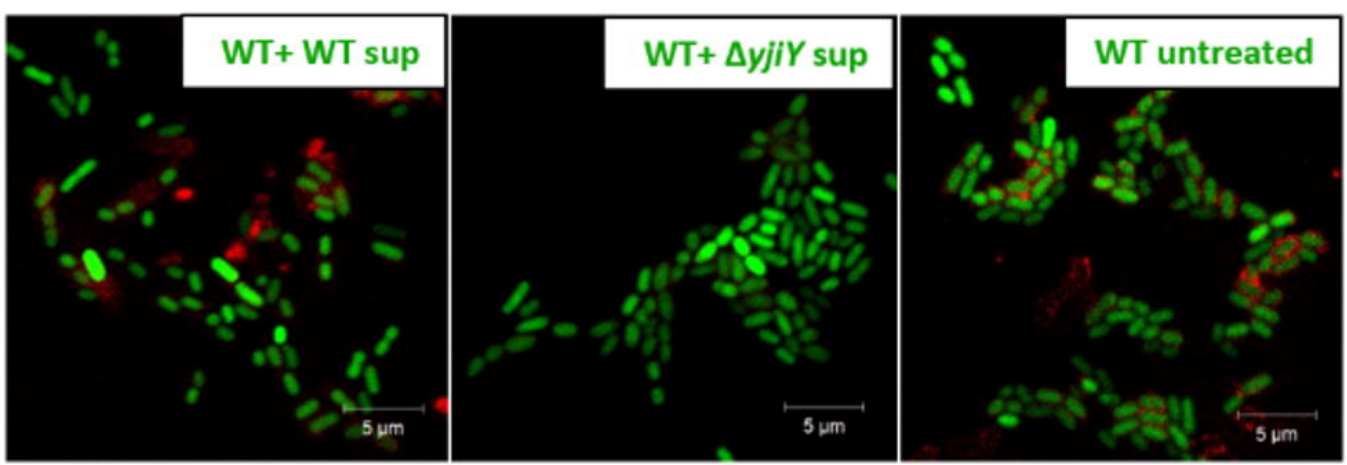
WT+ WT sup
WT+ ΔyjiY sup
WT untreated
5 μm
5 μm
5 μm

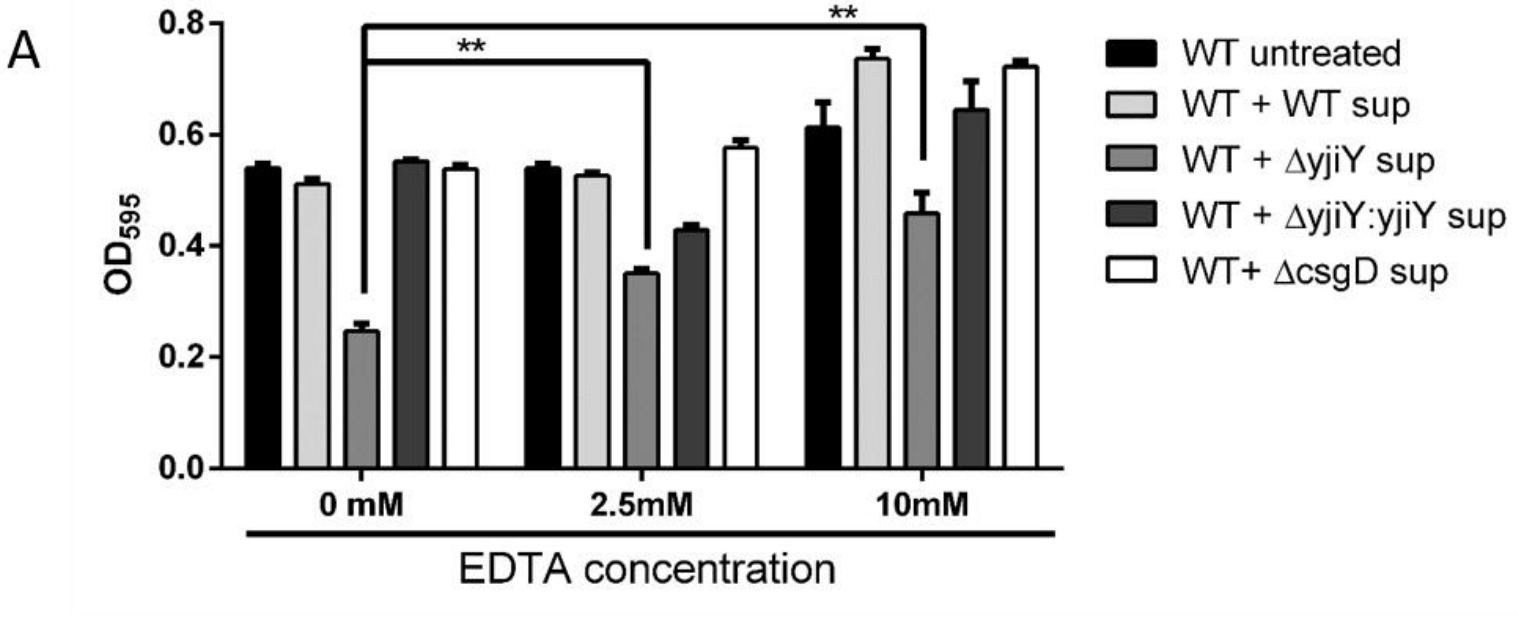
A
0.8
0.6
0.4
0.2
0.0
OD595
**
**
WT untreated
WT + WT sup
WT + ΔyjiY sup
WT + ΔyjiY:yjiY sup
WT+ ΔcsgD sup
0 mM
2.5mM
10mM
EDTA concentration

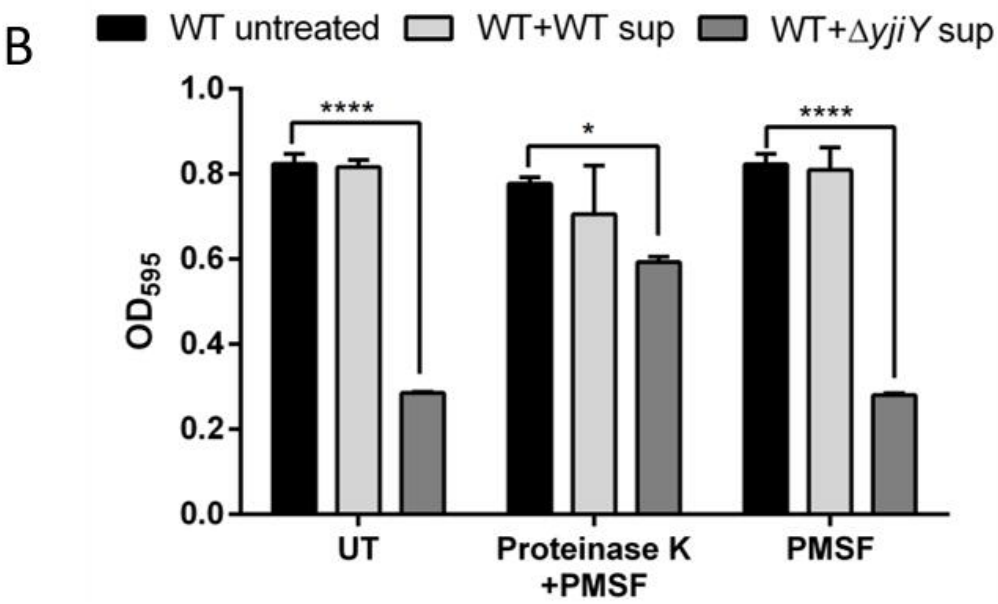
B
WT untreated
WT+WT sup
WT+ΔyjiY sup
1.0
0.8
0.6
0.4
0.2
0.0
OD595
****
*
****
UT
Proteinase K
+PMSF
PMSF

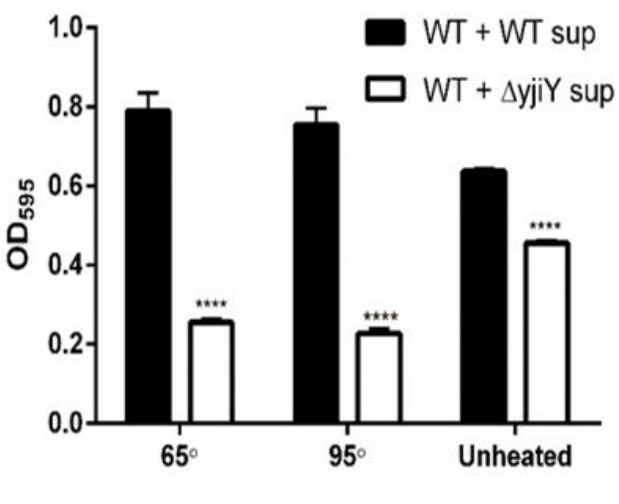
C
WT + WT sup
WT + ΔyjiY sup
1.0
0.8
0.6
0.4
0.2
0.0
OD595
****
****
****
65°
95°
Unheated

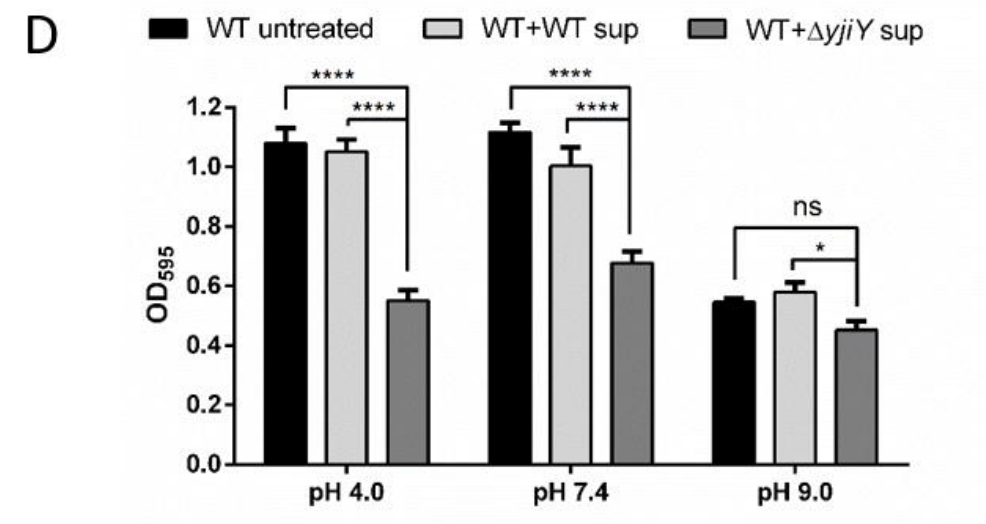
D
WT untreated
WT+WT sup
WT+ΔyjiY sup
1.2
1.0
0.8
0.6
0.4
0.2
0.0
OD595
****
****
****
****
ns
*
pH 4.0
pH 7.4
pH 9.0

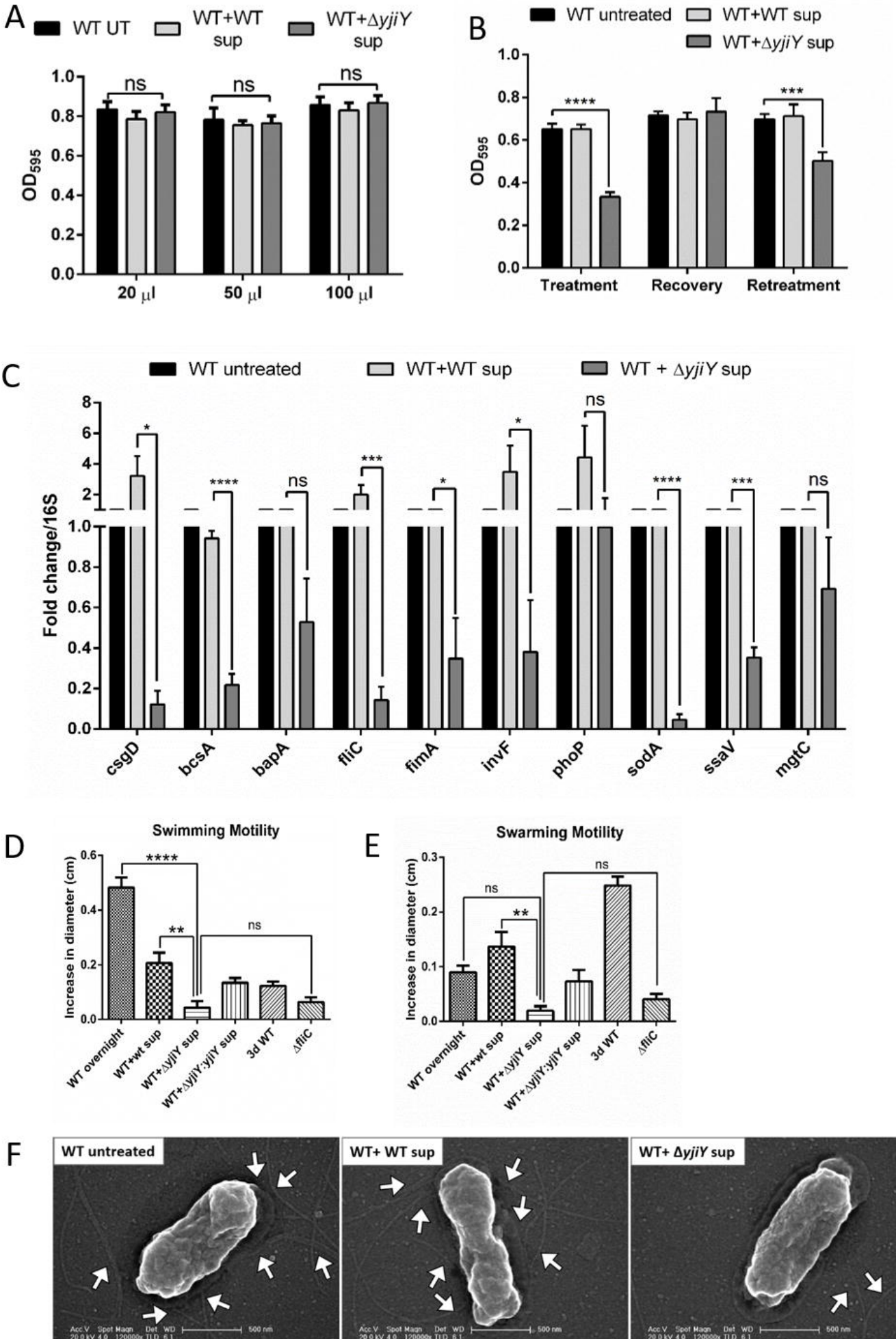
A
WT UT
WT+WT sup
WT+ΔyjiY sup
OD595
ns
20 µl
50 µl
100 µl
B
WT untreated
WT+WT sup
WT+ΔyjiY sup
OD595
****
***
Treatment
Recovery
Retreatment
C
WT untreated
WT+WT sup
WT + ΔyjiY sup
Fold change/16S
csgD
bcsA
bapA
fliC
fimA
invF
phoP
sodA
ssaV
mgtC
D
Swimming Motility
Increase in diameter (cm)
WT overnight
WT+wt sup
WT+ΔyjiY sup
WT+ΔyjiY:yjiY sup
3d WT
ΔfliC
E
Swarming Motility
Increase in diameter (cm)
F
WT untreated
WT+ WT sup
WT+ ΔyjiY sup

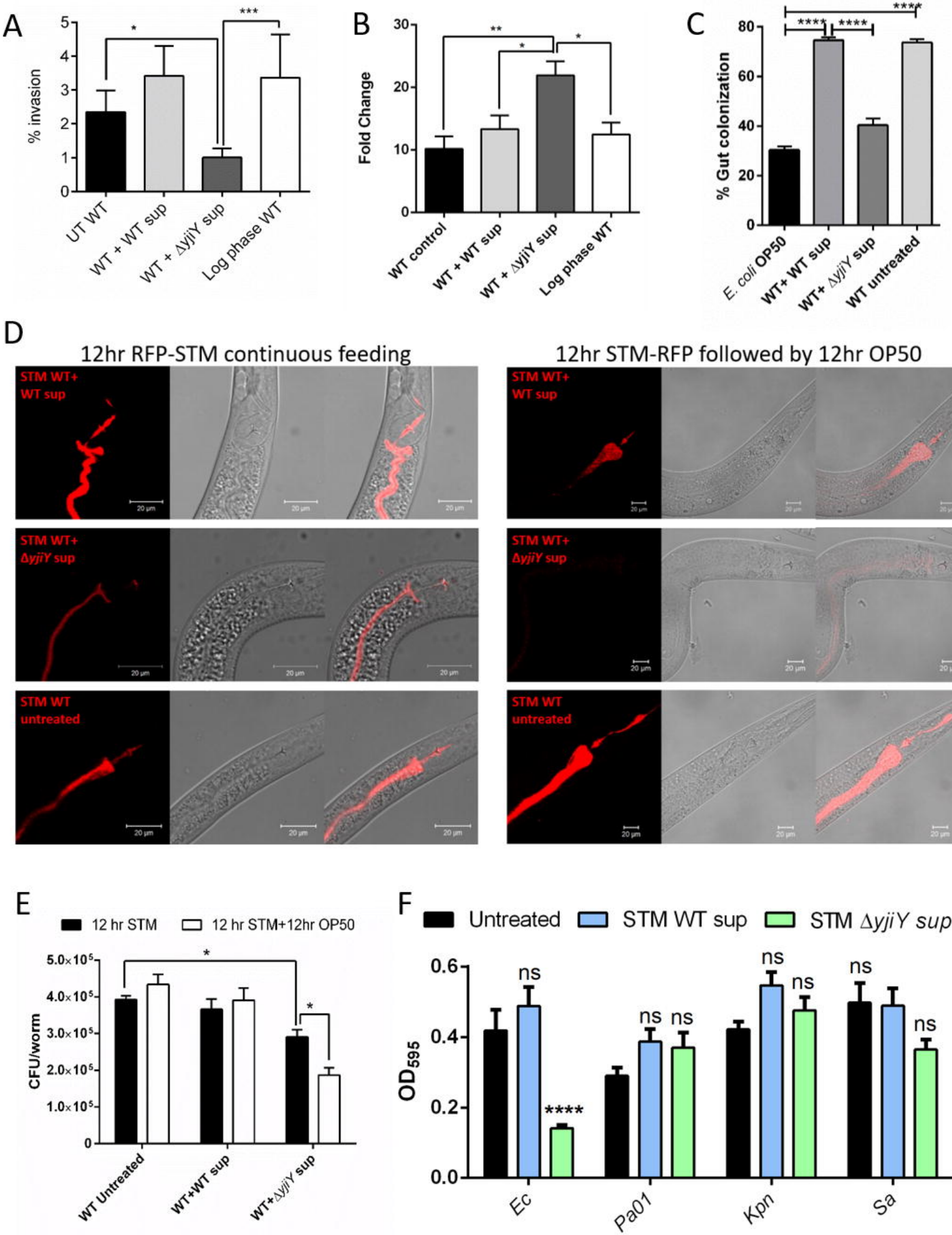
A
% invasion
UT WT
WT + WT sup
WT + ΔyjiY sup
Log phase WT
B
Fold Change
WT control
WT + WT sup
WT + ΔyjiY sup
Log phase WT
C
% Gut colonization
E. coli OP50
WT+ WT sup
WT+ ΔyjiY sup
WT untreated
D
12hr RFP-STM continuous feeding
12hr STM-RFP followed by 12hr OP50
STM WT+ WT sup
STM WT+ ΔyjiY sup
STM WT untreated
E
12 hr STM
12 hr STM+12hr OP50
CFU/worm
WT Untreated
WT+WT sup
WT+ΔyjiY sup
F
Untreated
STM WT sup
STM ΔyjiY sup
OD595
Ec
Pa01
Kpn
Sa

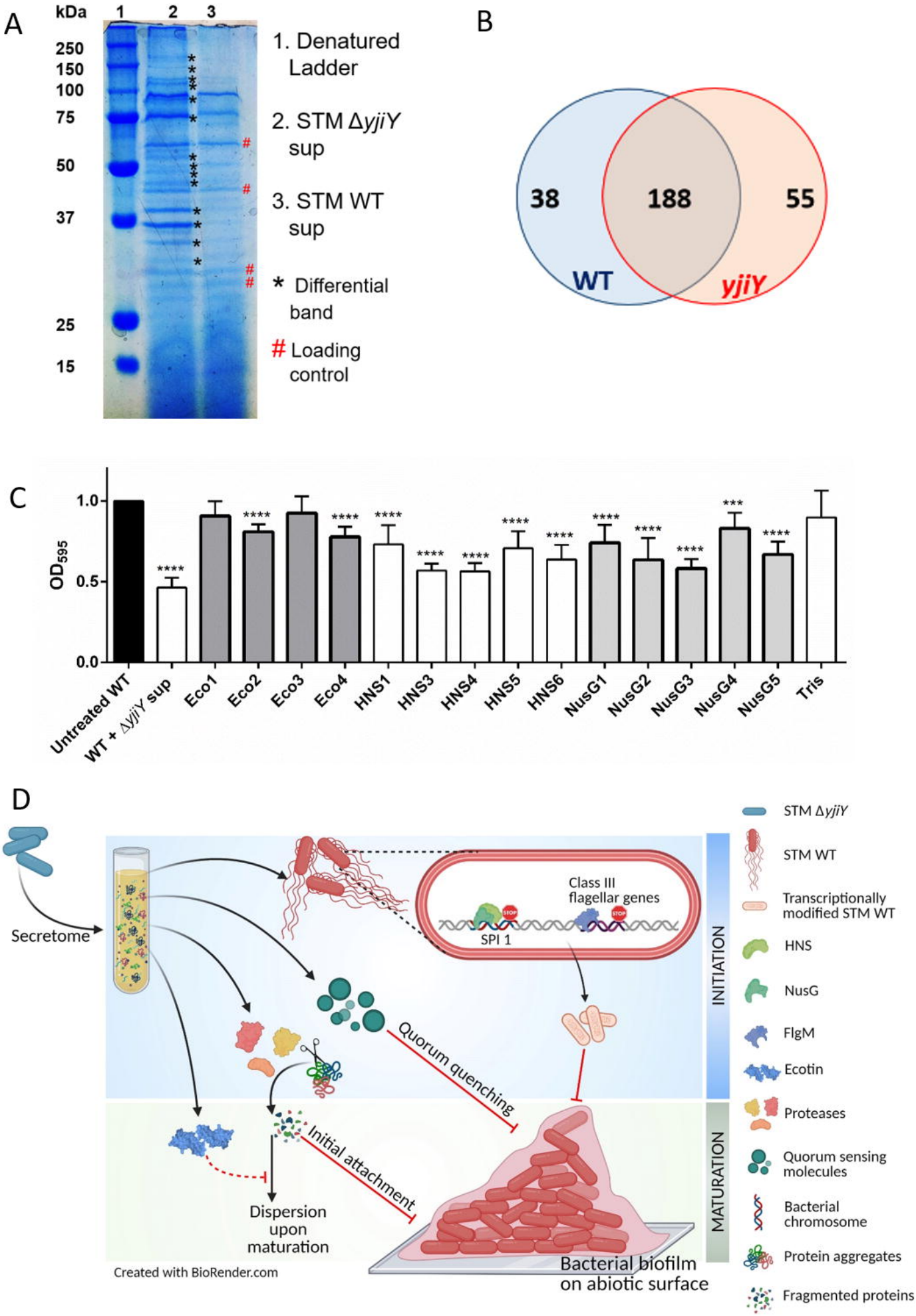
A
kDa
1
2
3
250
150
100
75
50
37
25
15
1. Denatured Ladder
2. STM ΔyjiY sup
3. STM WT sup
* Differential band
# Loading control
B
38
188
55
WT
yjiY
C
OD595
1.0
0.5
0.0
Untreated WT
WT + ΔyjiY sup
Eco1
Eco2
Eco3
Eco4
HNS1
HNS3
HNS4
HNS5
HNS6
NusG1
NusG2
NusG3
NusG4
NusG5
Tris
D
Secretome
Class III flagellar genes
SPI 1
Quorum quenching
Initial attachment
Dispersion upon maturation
Bacterial biofilm on abiotic surface
INITIATION
MATURATION
Created with BioRender.com
STM ΔyjiY
STM WT
Transcriptionally modified STM WT
HNS
NusG
FlgM
Ecotin
Proteases
Quorum sensing molecules
Bacterial chromosome
Protein aggregates
Fragmented proteins

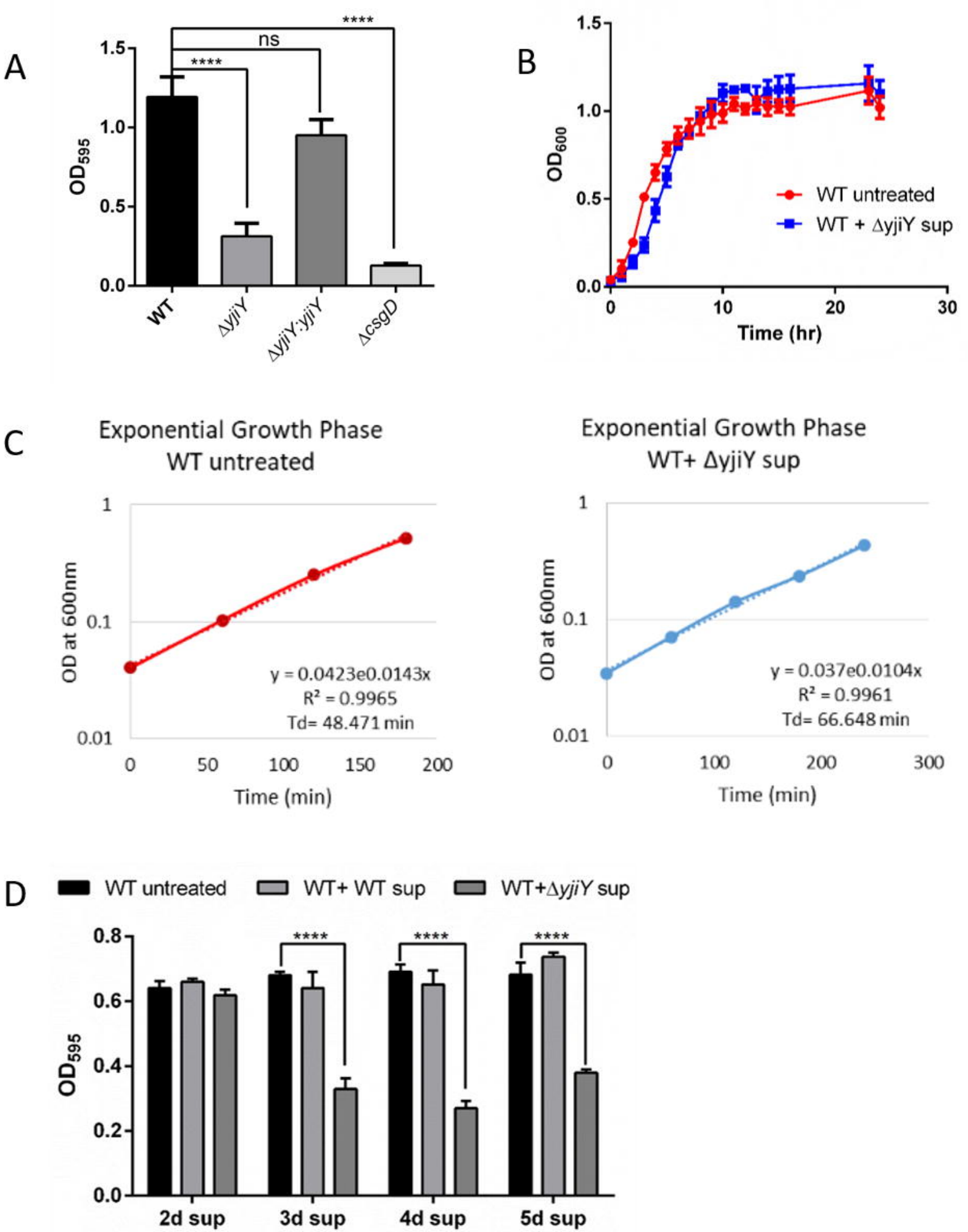
A
ns
****
****
1.5
1.0
0.5
0.0
OD595
WT
ΔyjiY
ΔyjiY:yjiY
ΔcsgD
B
1.5
1.0
0.5
0.0
OD600
0
10
20
30
Time (hr)
WT untreated
WT + ΔyjiY sup
C
Exponential Growth Phase
WT untreated
1
0.1
0.01
OD at 600nm
y = 0.0423e0.0143x
R² = 0.9965
Td= 48.471 min
0
50
100
150
200
Time (min)
Exponential Growth Phase
WT+ ΔyjiY sup
1
0.1
0.01
OD at 600nm
y = 0.037e0.0104x
R² = 0.9961
Td= 66.648 min
0
100
200
300
Time (min)
D
WT untreated
WT+ WT sup
WT+ΔyjiY sup
0.8
0.6
0.4
0.2
0.0
OD595
****
****
****
2d sup
3d sup
4d sup
5d sup

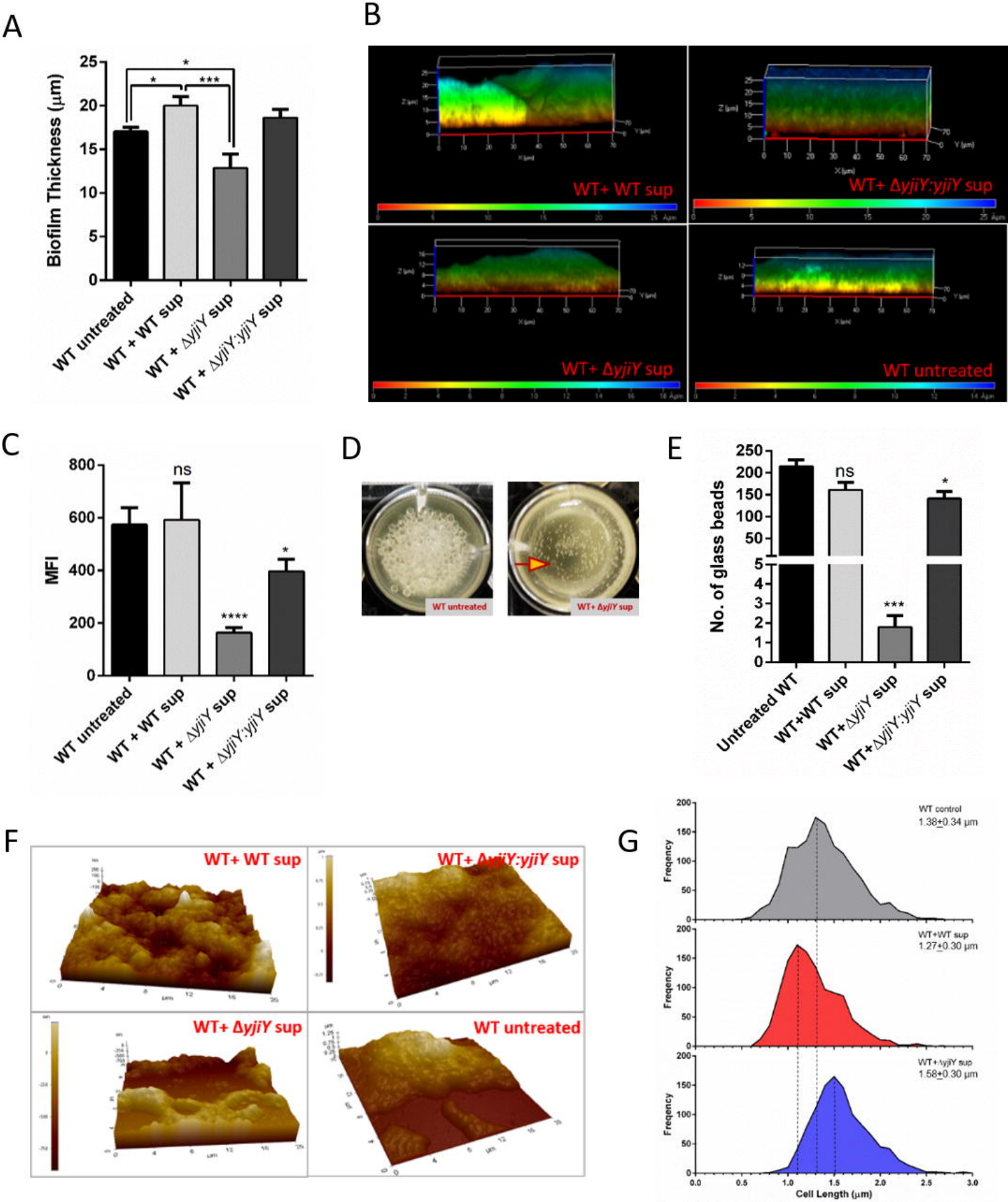
A
Biofilm Thickness (μm)
25
20
15
10
5
0
*
*
***
WT untreated
WT + WT sup
WT + ΔyjiY sup
WT + ΔyjiY:yjiY sup
B
WT+ WT sup
WT+ ΔyjiY:yjiY sup
WT+ ΔyjiY sup
WT untreated
C
MFI
800
600
400
200
0
ns
****
*
WT untreated
WT + WT sup
WT + ΔyjiY sup
WT + ΔyjiY:yjiY sup
D
WT untreated
WT+ ΔyjiY sup
E
No. of glass beads
250
200
150
100
50
5
4
3
2
1
0
ns
***
*
Untreated WT
WT+WT sup
WT+ΔyjiY sup
WT+ΔyjiY:yjiY sup
F
WT+ WT sup
WT+ ΔyjiY:yjiY sup
WT+ ΔyjiY sup
WT untreated
G
Freqency
WT control
1.38±0.34 μm
WT+WT sup
1.27±0.30 μm
WT+ΔyjiY sup
1.58±0.30 μm
0.0
0.5
1.0
1.5
2.0
2.5
3.0
Cell Length (μm)

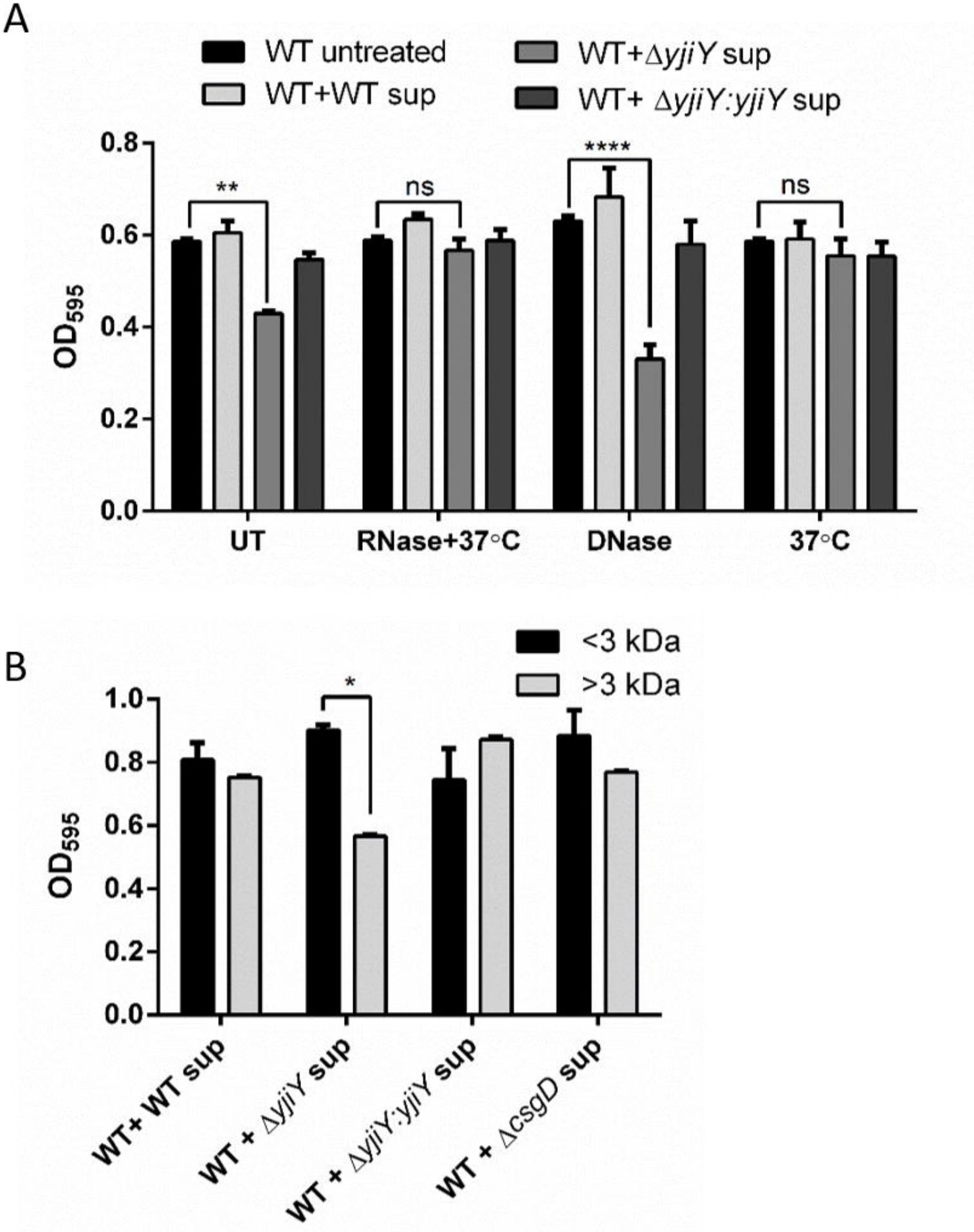
A
WT untreated
WT+WT sup
WT+ΔyjiY sup
WT+ ΔyjiY:yjiY sup
OD595
0.0
0.2
0.4
0.6
0.8
**
ns
****
ns
UT
RNase+37°C
DNase
37°C
B
<3 kDa
>3 kDa
OD595
0.0
0.2
0.4
0.6
0.8
1.0
*
WT+ WT sup
WT + ΔyjiY sup
WT + ΔyjiY:yjiY sup
WT + ΔcsgD sup

A

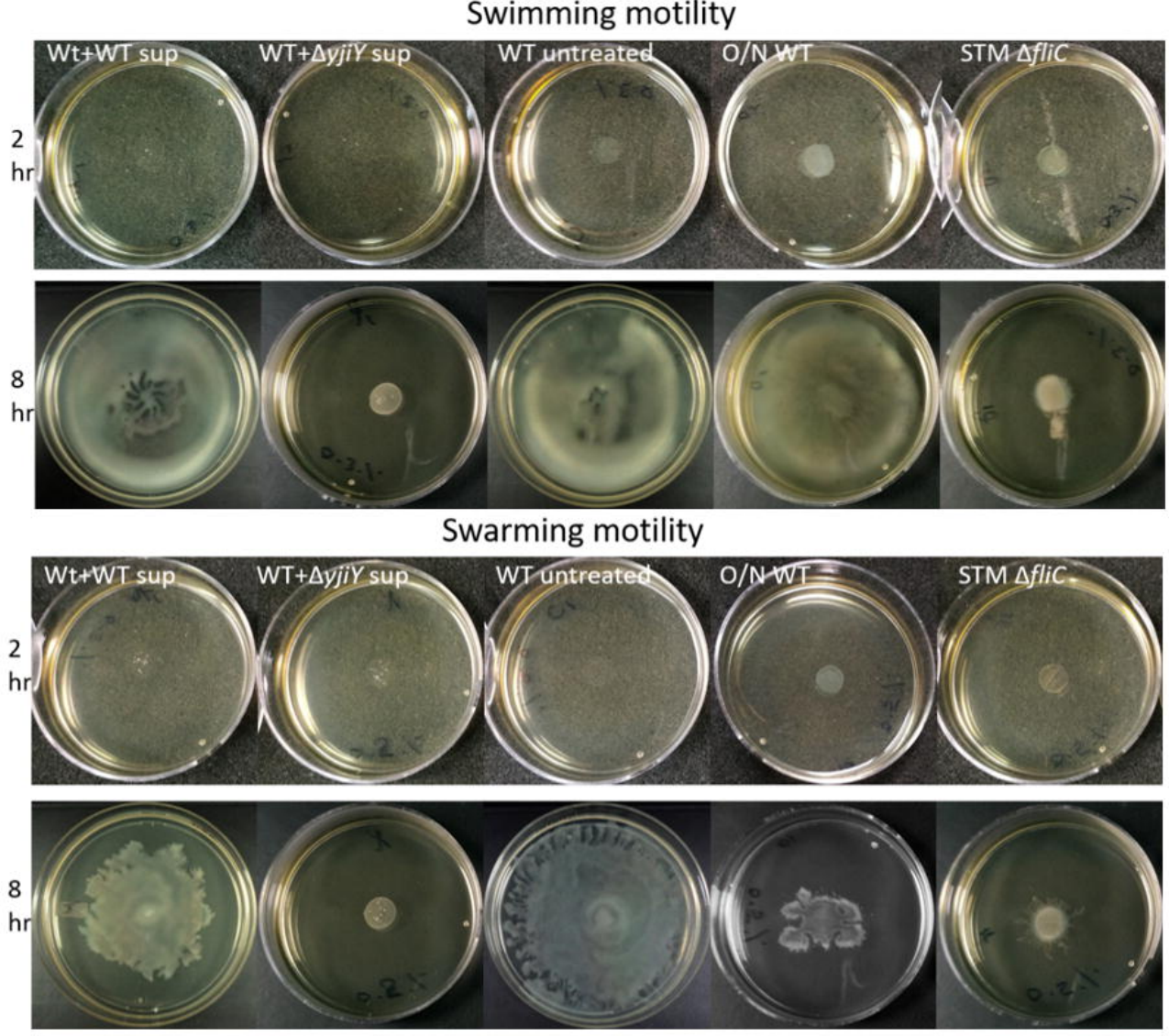
Swimming motility
Wt+WT sup
WT+ΔyjiY sup
WT untreated
O/N WT
STM ΔfliC
2 hr
8 hr
Swarming motility
Wt+WT sup
WT+ΔyjiY sup
WT untreated
O/N WT
STM ΔfliC
2 hr
8 hr

B

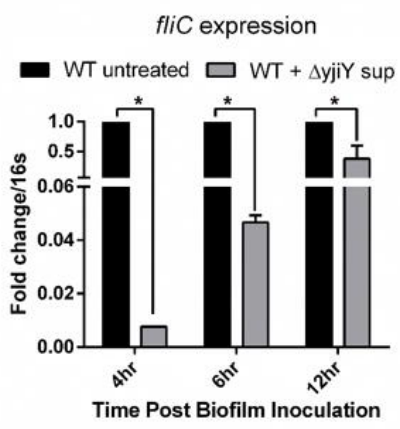
fliC expression
WT untreated
WT + ΔyjiY sup
Fold change/16s
1.0
0.5
0.06
0.04
0.02
0.00
4hr
6hr
12hr
Time Post Biofilm Inoculation

C

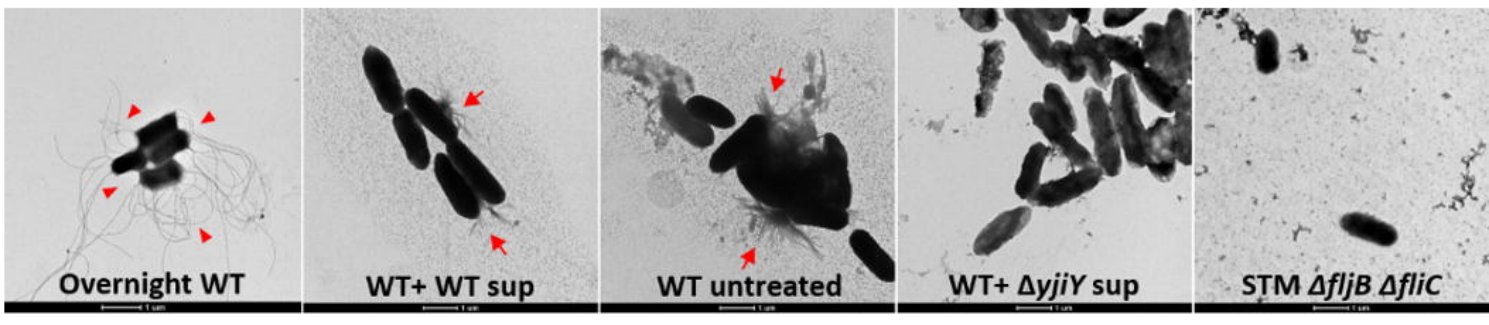
Overnight WT
WT+ WT sup
WT untreated
WT+ ΔyjiY sup
STM ΔfljB ΔfliC

Ladder
Lysate
FT
Pellet
100mm
150mM
200mM
250mM
300mM
350mM
400mM
450mM
500mM
Wash 1
Wash 5
(Ecotin)
19 kDa
17 kDa

Lysate
FT
Ladder
100mM
200mm
300mM
400mM
500mM
600mM
700mM
800mM
900mM
1000mM
Wash 1
Wash 5
17 kDa
16.3 kDa
(HNS)

Ladder
Lysate
FT
100mM
200mm
300mM
400mM
500mM
600mM
700mM
800mM
900mM
1000mM
Wash 1
Wash 5
25 kDa
21.3 kDa
(NusG)

A

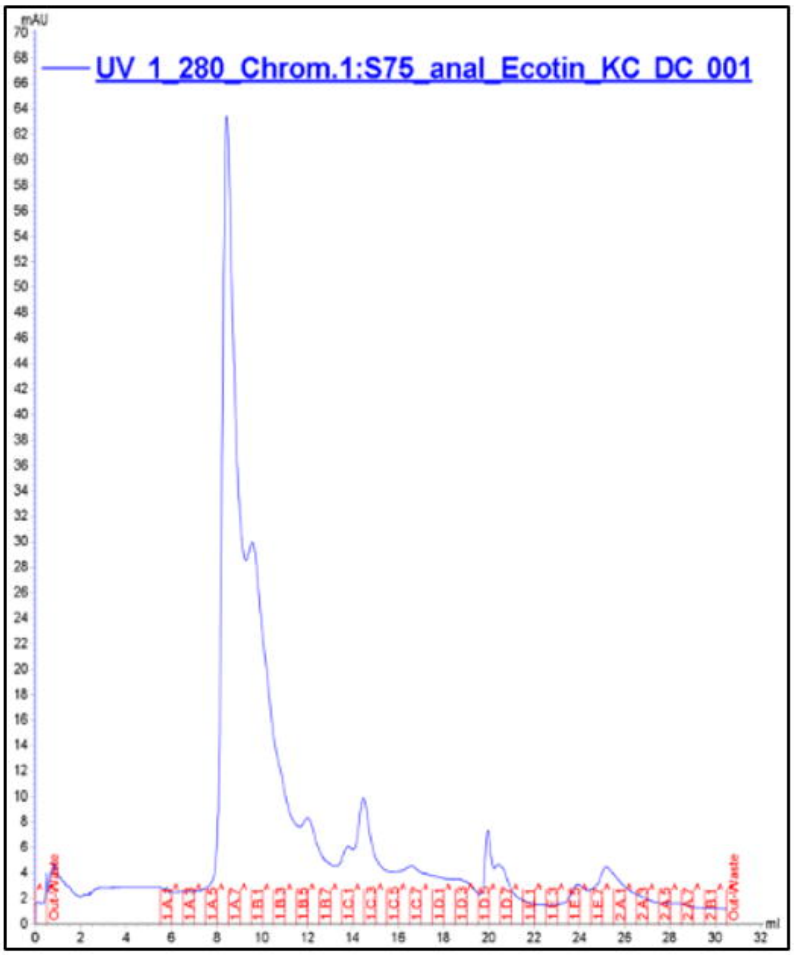

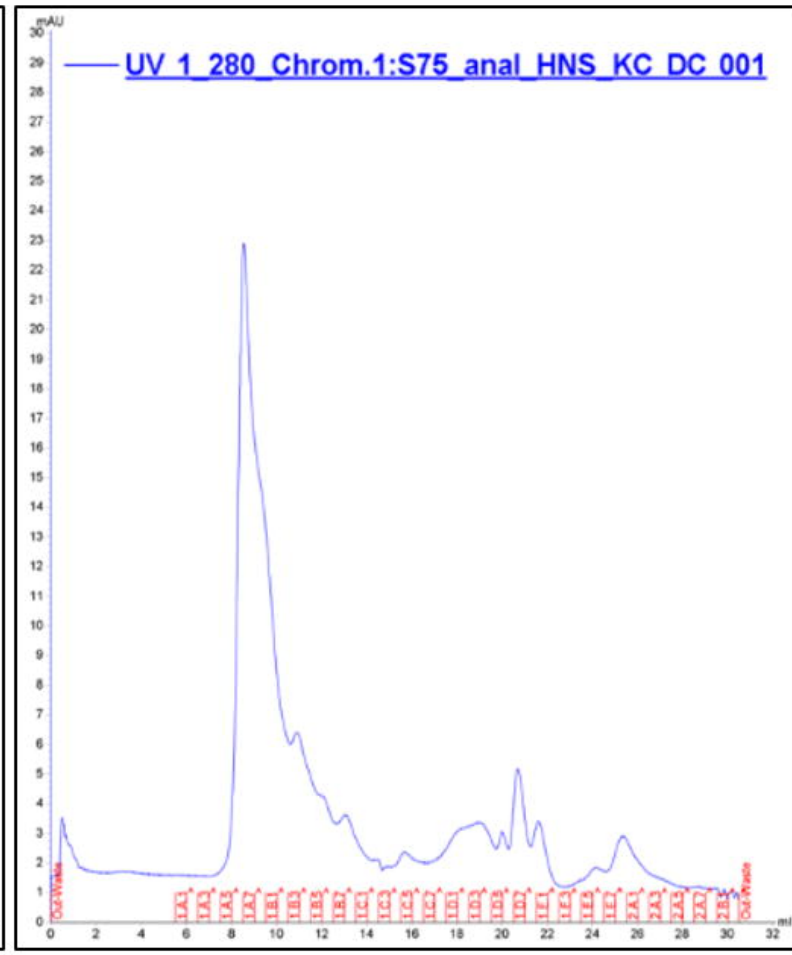

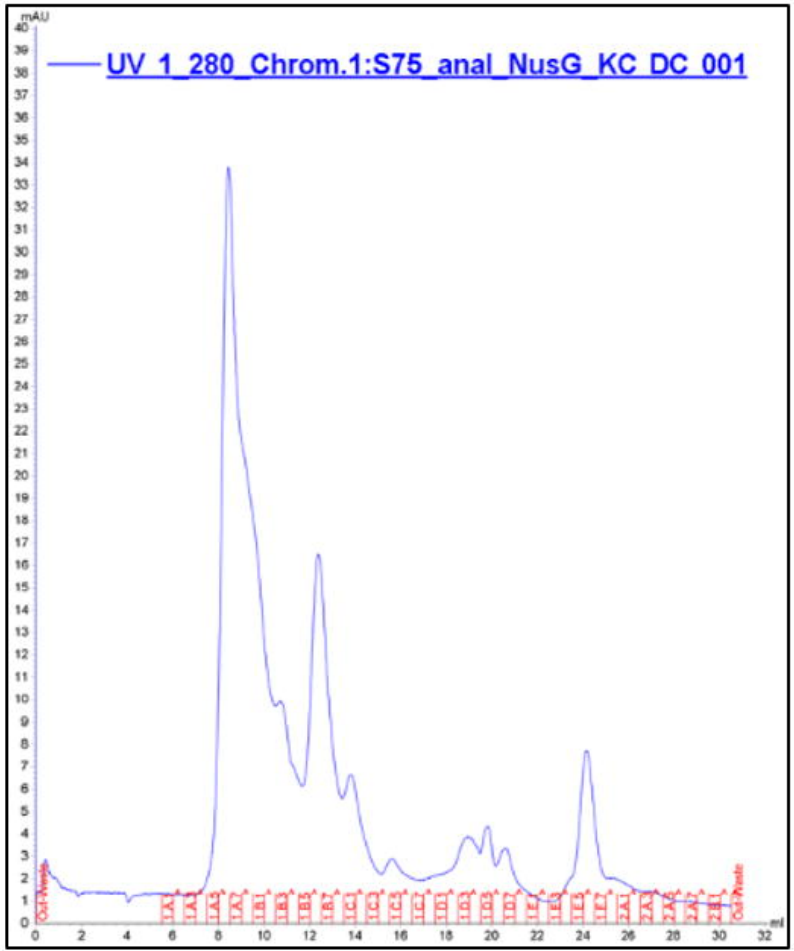

B

Protein Name	Fraction Name	Pooled Fractions	Elution Volume (ml)	Oligomeric State
Ecotin	E1	A6, A7, A8	8-9	Homodimer
	E2	B1, B2, B3, B4	10-11	
	E3	B5, B6, B7	12-13	Monomer
	E4	C2, C3	14-15	
HNS	H1	A6, A7, A8, B1	8-9	Heterotrimer (Hha)
	H3	B3, B4	11	Homodimer
	H4	B5, B6	12-13	
	H5	B7, B8	13-14	Monomer
	H6	C4, C5, C7	15-17	
NusG	N1	B2	10-10.5	Monomer
	N2	B3	10.5-11	
	N3	B4	11-11.5	
	N4	B6, B7, B8	12-13.5	
	N5	C1, C2	13.5-14.5	